JPET Fast Forward. Published on August 24, 2007 as DOI: 10.1124/jpet.107.129551

JPET #129551

Activity-dependent neuroprotective protein snippet NAP reduces tau hyperphosphorylation and enhances learning in a novel transgenic mouse model

Inna Vulih-Shultzman, Albert Pinhasov, Shmuel Mandel, Nikolaos Grigoriadis, Olga Touloumi, Zipora Pittel, and Illana Gozes

Department of Human Molecular Genetics and Biochemistry, Sackler School of Medicine, Tel Aviv University, Tel Aviv 69978, Israel (I.V.S., A.P., S.M., Z.P., I.G.); and Dept of Neurology and Lab of Experimental Neurology, AHEPA University Hospital, Aristotle University of Thessaloniki, Stilp. Kyriakidi str 1, GR-54636 Thessaloniki, Greece (N.G., O.T.)

Running Title: NAP affects tau and learning in a novel transgenic model

Corresponding Author: Prof. Illana Gozes,

Department of Human Molecular Genetics and Biochemistry,

Sackler School of Medicine,

Tel Aviv University,

Tel Aviv 69978,

Israel.

Telephone: 972-3-640-7240; FAX: 972-3-640-8541;

E-mail: igozes@post.tau.ac.il

The number of text pages: 41

The number of tables: 0

The number of figures: 6

The number of references: 40

The number of words in the abstract: 143

The number of words in the introduction: 473

The number of words in the discussion: 1303

Nonstandard abbreviations used in the paper: ADNP, activity-dependent neuroprotective protein**;** GSK3β, glycogen synthase kinase-3β; ADNP+/-, heterozygous; ADNP+/+, wild type.

Recommended section assignment: Neuropharmacology

Abstract

Activity-dependent neuroprotective protein (ADNP) differentially interacts with chromatin to regulate essential genes. As complete ADNP deficiency is embryonic lethal, the outcome of partial ADNP deficiency was examined. ADNP+/- mice exhibited cognitive deficits, significant increases in phosphorylated tau, tangle-like structures and neurodegeneration as compared to ADNP+/+ mice. Increased tau hyperphosphorylation is known to cause memory impairments in neurodegenerative diseases associated with tauopathies, including the most prevalent Alzheimer's disease. The current results suggest that ADNP is an essential protein for brain function and plays a role in normal cognitive performance. ADNP-deficient mice offer an ideal paradigm for evaluation of cognitive enhancers. NAP (NAPVSIPQ) is a peptide derived from ADNP that interacts with microtubules and provides potent neuroprotection. NAP treatment partially ameliorated cognitive deficits and reduced tau hyperphosphorylation in the ADNP+/- mice. NAP is currently in phase II clinical trials assessing effects on mild cognitive impairment.

JPET Fast Forward. Published on August 24, 2007 as DOI: 10.1124/jpet.107.129551
This article has not been copyedited and formatted. The final version may differ from this version.

Introduction

Activity-dependent neuroprotective protein (ADNP, ~124KDalton) (Bassan et al., 1999; Zamostiano et al., 2001) is essential for brain development (Pinhasov et al., 2003). The highly conserved ADNP gene (Zamostiano et al., 2001) is abundantly expressed in the hippocampus (Bassan et al., 1999), cerebral cortex (Bassan et al., 1999; Zamostiano et al., 2001) and cerebellum (Zamostiano et al., 2001) and is modulated by injury (Zaltzman et al., 2004; Gozes et al., 2005b) and hormonal activity (Furman et al., 2005). Inhibition of ADNP expression results in cancer cell death (Zamostiano et al., 2001) and recombinant ADNP exhibits protection against severe oxidative stress in a neuronal cell model (Steingart and Gozes, 2006).

The deduced protein structure of ADNP contains nine zinc fingers, a proline-rich region, a nuclear bipartite localization signal, and a homeobox domain profile, implying a transcription factor function (Zamostiano et al., 2001). Affymetrix microarrays were used on ADNP knockout and control mouse embryos to reveal marked differences in expression profiles. A group of dramatically up-regulated gene transcripts in the ADNP-deficient embryos clustered into a family encoding for proteins associated with metabolism such as apolipoproteins, cathepsins and metallothioneins and a down-regulated gene cluster was associated with neurogenesis (*Ngfr*, *neurogenin1*, *neurod1*) and heart development (*Myl2*) (Mandel et al., 2007).

Within its homeobox profile, ADNP contains a nuclear export signal and an import signal, signifying possible extracellular functions. Furthermore, a potential interaction with cytoplasmic microtubules has been observed (Furman et al., 2004). Structure-activity studies identified a short peptide sequence in ADNP, NAP (NAPVSIPQ), that mimics the neuroprotective activity of the parent protein and crosses the blood brain barrier after systemic or intranasal administration (Gozes et al., 2005a). Importantly, NAP interacts with tubulin and

enhances microtubule assembly (Divinski et al., 2004) to increase neurite outgrowth and to specifically protect neurons and glial cells against severe toxicities (Divinski et al., 2006). *In vitro*, NAP was found to reduce tau hyperphosphorylation (Gozes and Divinski, 2004) that has been associated with neurodegeneration/tauopathy and cognitive decline *in vivo* (Modrego, 2006). Two different lines of investigation were taken to ascertain specificity for NAP activity. Firstly, a scrambled NAP peptide was used in neurite outgrowth experiments in hippocampal cell *in vitro* showing essentially loss of activity (Smith-Swintosky et al., 2005). Secondly, NAP administration to rabbits (Gozes et al., 2005a) and repeated administration to rodents (Allon Therapeutics, personal communication) did not elicit any immune response. Based on these results and a clean toxicology profile, NAP is currently in phase II clinical trials targeting cognitive impairments (Allon Therapeutics Inc.).

As the homozygous ADNP knockout phenotype was found to be embryonic lethal (Pinhasov et al., 2003), the goal was set to assess the heterozygous phenotype, in order to obtain a better understanding of neuroprotection in association with reduced expression of ADNP and to evaluate the potential ameliorative value of NAP therapy in an *in vivo* ADNP deficient model.

Methods

Animals. All procedures involving animals have been approved by the Animal Care and Use Committee of Tel Aviv University and of the National Institutes of Health, Bethesda, MD, USA. ADNP heterozygous mice (Pinhasov et al., 2003) were housed in a 12-h light and 12-h dark cycle facility and free access to rodent chow and water was available.

ADNP +/- mice generation procedure. The procedure to generate ADNP+/- animals was described (Pinhasov et al., 2003). In short, a bacterial artificial chromosome (pBeloBAC11, 7.3kb) 129Sv mouse library was screened (Genome Systems Inc. St. Louis, Mo., USA) and a BAC clone containing the mouse ADNP gene, was isolated. The X-pPNT vector (8231 bp) was used to generate a targeting vector for the ADNP gene. To construct the targeting vector, exons III, IV, and V of the ADNP gene and their adjacent introns were replaced with the neomycin resistance gene. Flanking regions of the ADNP gene, 3.3 kb from the 5' end and 3 kb from the 3' end, were preserved. A Herpes Simplex virus thymidine kinase gene was cloned 3' of the targeting insert as a negative selection marker. The final targeting vector was 14 kb long. The linearized targeting vector was transfected into embryonic stem cells derived from 129/sv mouse for homologous recombination. Targeted positive clones were double selected with G418 and gancyclovir and screened by Southern blot hybridisation outside the flanking homologous sequences. Positive clones were microinjected into C57BL/6-derived blastocysts, and gave rise to chimaeric offspring that carried the mutation into the germ line. Chimera males transmitted the mutation on breeding with C57BL/6 female mice. Generated heterozygous mice were subsequently crossed to produce ADNP+/+, ADNP+/- and knockout (ADNP-/-) progeny. The knockout progeny (ADNP-/-) is embryonic lethal (Pinhasov et al., 2003).

Genotyping. Genomic DNA was extracted from mouse tails. Lysis buffer (100 mM Tris HCl pH 8.5, 5mM EDTA, 0.2% SDS, 200 mM NaCl, proteinase K 0.35 mg/ml) was added to each sample followed by a 16hr incubation period at 37°C and vigorous mixing. Genomic DNA was then precipitated by isopropanol, washed by 70% ethanol, dissolved in TE buffer (10 mM Tris-HCl, pH 8, 100 µM EDTA) and subjected to PCR for genotyping.

NAP treatment. NAP (NAPVSIPQ, Allon Therapeutics, Inc.) was injected to newborn mice over a two week period. NAP was diluted to a final concentration of 25 µg/ml saline before injection (Bassan et al., 1999). Daily subcutaneous injections included 20 µl, 0.5 µg/mouse/day (days 1–4), 40 µl, 1 µg/mouse/day (days 5–10), and 80 µl, 2 µg/mouse/day (days 11–14), exact saline quantities were injected to control mice. At the age of two months, male mice were subjected to behavioral testing (see below). In a separate experiment, NAP treatment included daily intranasal administrations over a two week period to 2 month-old male mice and to nine month-old male mice (0.5 µg/5 µl/mouse/day). For intranasal administration, the peptide was dissolved in a solution, DD, in which each milliliter included 7.5 mg of NaCl, 1.7 mg of citric acid monohydrate, 3 mg of disodium phosphate dihydrate and 0.2 mg of benzalkonium chloride solution (50%) (Alcalay et al., 2004). NAP or vehicle solution (DD) was administered to mice hand held in a semi- supine position with nostrils facing the investigator. A pipette tip was used to administer 2.5 µl/each nostril. The mouse was hand held until the solution was totally absorbed (~10 seconds). Nasal NAP application was performed daily, once a day, for two weeks (5 days a week). On the second week, NAP was applied one hour prior to the daily Morris water maze test (see below), which was conducted for 5 consecutive days.

Gene array. All experiments were performed using Affymetrix MOE430A oligonucleotide arrays, as described in http://www.affymetrix.com/products/arrays/specific/mouse430a_2.affx. The precise experimental details for the ADNP+/- embryos are outline in a previous study (Mandel et al., 2007). In short, total RNA was extracted from four ADNP knockout embryos, four normal embryos and six heterozygous embryos completely devoid of extra embryonic tissue. A pool of two genotype-identical littermates was used on seven different arrays (pooling of two embryos was necessary to obtain sufficient RNA for the microarray analysis). Gene expression results were analyzed using the novel Expander software as before. From the 22,690 probes on the array, only 13,814 showed a significant signal (i.e. were present on the array and showed expression intensity >20 arbitrary units) indicating that these genes were expressed at the E9 stage of embryonic development.

Tissue culture experiments. Experiments were conducted with mixed neuronal glial cultures that were obtained from newborn mouse cerebral cortex (ADNP+/+ and ADNP+/-) that were used as support cells to neuronal cells obtained from newborn rat brains as before (Bassan et al., 1999; Divinski et al., 2006). Neuronal survival was evaluated by direct neuronal counting (Bassan et al., 1999; Divinski et al., 2006).

All experiments described below were performed on male mice.

RNA isolation. Total RNA was isolated from frozen brains using the TriPure reagent (Boehringer Mannheim, Germany) and/or the Qiagene RNeasy mini kit (Quiagene, Hilden, Germany).

Reverse transcription and quantitative real time polymerase chain reaction (RT-quantitative PCR). Total RNA was treated by DNaseI (Ambion, Austin, TX) and 1µg

RNA/sample was reverse-transcribed by SuperScript III reverse transcriptase (100 U, Invitrogen, Carlsbad, CA) using oligo(dT)18 primers (1h at 50°C, 10 min at 75°C). Real-time RT-PCR was performed using FastStart DNA Master SYBR Green 1 dye-base detection kit (Roche Diagnostics Mannheim, Germany). A Light Cycler instrument was used with its internal relative quantification software (Roche Diagnostics Mannheim, Germany), which utilizes melting point analysis to assess the specificity of the amplified genes. All reactions were performed with a magnesium chloride concentration of 2.5 mM, primer concentrations of 0.05 μM, and 2.5 μl of the reverse transcription product in a 10 μl reaction mixture. Annealing temperature was 60°C for the ADNP transcript and for the internal mRNA standard, encoding the ribosomal protein L19 Primer sequences for PCR analyses were according to previous publications (Mandel et al., 2007). The ADNP mRNA primers were sense 5'CGAAAAATCAGGACTATCGG3', and antisense 5'TGAAAGTGCTGAGGCTGCTA3'. The Pax6 primers used (a kind gift from Dr. Ruth Asheri-Padan) were: sense 5'ACTCCACCCGGCAGAAGATC3' and antisense 5'CCAGTCTCGTAATACCTGCCC3'.

Protein isolation. Mice were sacrificed by cervical dislocation. The cerebral cortex was isolated from each brain, weighed and homogenized in 10 volumes of ice-cold lysis buffer (10mM Tris-HCl, 150mM NaCl, 20mM NaF, 1mM Na_3VO_4, 2mM EGTA, 0.5% Triton-X 100 and 0.1% SDS) containing a protease inhibitor cocktail (Sigma, Saint Louis, USA). The suspended tissue was then sonicated using an ultrasonic cell disrupter (Microson™, Misonix Inc. Farmingdale, NY, USA). The resulting homogenate was centrifuged (3000 g, 20 min, 4^0C), the supernatant was then collected and protein concentrations were determined by BCA-200 protein assay kit (Pierce, Rockford, IL, USA).

JPET Fast Forward. Published on August 24, 2007 as DOI: 10.1124/jpet.107.129551
This article has not been copyedited and formatted. The final version may differ from this version.

Western blot analysis. Proteins (15 μg/lane) of the resulting supernatant (above) were separated by electrophoresis on a 10% polyacrylamide gel and electrotransfered to nitrocellulose filters followed by Western blot analysis (Zamostiano et al., 2001). Nonspecific antigen sites were blocked using a solution containing 5% non-fat dried milk (w/v) in 10 mM Tris pH 8, 150 mM NaCl and 0.05% Tween 20. For ADNP detection, the rabbit polyclonal ADNP antibody (BL1034, Bethyl Laboratories, Inc. Montgomery, Tx, USA) was used. The epitope recognized by this antibody maps to a region between residues 1050-1102 (C-terminal) of ADNP (Zamostiano et al., 2001). Other antigens were detected using the following antibodies: 1] monoclonal (PHF-tau, AT-8, Innogenetics, Alpharetta, GA, USA); 2] polyclonal (Anti-Tau [pT^{231}], Biosource, Camarillo, CA, USA; AT180); both are mouse antibodies recognizing phosphorylated tau; 3] mouse monoclonal TAU-5 antibody that recognizes total tau (reacts with the non-phosphorylated as well as the phosphorylated forms of tau; Biosource); 4] polyclonal antibody to phosphor-GSK3α/β (pTyr279/216); 5] anti-GSK-3β [pS^{9}], purchased from Biosource (Camarillo, CA, USA); and 6] monoclonal mouse actin antibodies (ImmunO, Aurora, Ohio, USA). Peroxidase-conjugated affinity pure goat anti-mouse (Jackson Immuno Research Laboratories. Inc., West Grove, PA, USA) and anti-rabbit IgG secondary antibodies (Sigma, Rehovot, Israel) were visualized by ECL Plus detection system (Amersham Biosciences, Buckinghamshire, UK). The ADNP antibody was diluted at 1:3000; the AT-8 antibody was used at a dilution of 1:500 whereas other primary antibodies were diluted at 1:1000. The secondary anti-mouse antibody was used at a dilution of 1:10,000 and the secondary anti-rabbit antibody was used at a dilution of 1:25,000.

Assessment of short-term spatial memory in a water maze. Male mice were subjected to two daily tests in a water maze, including a hidden platform (Gozes et al., 2000). Water

temperature was maintained at 23-240C, bath water was changed every day and water was made opaque by the addition of dry milk powder. Maximum duration of each daily test for each mouse (two daily trials) was 180 seconds. Every day for the first test, both the platform and the animal were situated in a new location with regards to the pool (with the pool being immobile). The experiment was performed as follows: the animal was positioned on the platform for 0.5 min then placed in the water. The time required to reach the platform (indicative of learning and intact reference memory) was measured (first test). After 0.5 min on the platform, the animal was placed back in the water (in the previous position) for a second test and search for the hidden platform (retained in the previous position). The time required to reach the platform in the second trial was recorded, indicative of short-term (working) memory. A maximal exploration time of 90 second per trial was allocated to each test. To avoid bias related to changes in motor activity in the various treatment groups the last test included a visible platform trial that was performed 2 hours after the previous test. Measurements were performed with the HVS video tracking system (HVS Image Ltd., Hampton, UK).

Assessment of motor behavior. Tests were performed in an open field – 80 cm in diameter. Each male mouse (2 or 9 month old) was placed in the middle of the field and path traveled was measured the imaging system (above) for three minutes or one hour.

Social recognition. The social recognition test, based on the social memory test of Thor and Holloway as reproduced by Hill and colleagues (Hill et al., 2007), assessed the time a male mouse spent sniffing and following an unfamiliar female mouse during repeated presentations at 30 min intervals. Four three-month-old male control mice (ADNP+/+) and three three-month-old ADNP+/- mice were tested individually by introducing them into a clean mouse cage containing an unfamiliar aged (18 month old) female mouse (Female 1). Over a 5 min period,

the experimenter recorded the amount of time the male mouse sniffed and followed the female mouse. The mice were then separated for 30 min followed by a second pairing of 5 min during which the amount of time the male mouse sniffed and followed the female mouse was recorded. This was repeated 3 more times at 30 min intervals. After 5 pairings with the same ovariectomized female, the male was then paired with an unfamiliar aged (18 month old) female mouse (Female 2) and the amount of time spent sniffing and following the unfamiliar female was recorded.

Tissue preparation for histology and immunohistochemistry. Male mice 5-11 months of age were perfused transcardially under deep anesthesia with 4% paraformaldehyde in 0.1M phosphate buffered saline (PBS), pH 7.4. The brains were removed and further cut along the midline. The two brain hemispheres were dissociated and placed in the same fixative at 4°C for 4 hours and then immersed in 30% sucrose in PBS pH 7.4 for cryoprotection. Brain hemispheres, in pairs, were frozen on block and serial sagittal cryostat sections, 8μm thick, were cut at 5 levels, 200 μm apart, initiating from the inner interface of each hemisphere and mounted on glass slides (Superfrost Plus).

Histology – Immunohistochemistry. A number of sections from each brain level were subjected to hematoxylin-eosin (H-E) staining for the identification of morphological changes. Adjacent sections were stained with Fluoro-Jade B, a fluorescent chromofluor that selectively labels degenerating neurons (Anderson et al., 2005). Briefly, the slides were first immersed in a solution containing 1% sodium hydroxide in 80% alcohol for 5 min. This was followed by 2 min in 70% alcohol and 2 min in distilled water. The slides were then transferred to a solution of 0.06% potassium permanganate for 10 min on a shaker table to ensure consistent background suppression between sections and further rinsed in distilled water for 2 min. The staining solution

was prepared from a 0.01% stock solution of Fluoro-Jade B (Chemicon, Temecula, CA, USA) in 0.1% acetic acid vehicle in a concentration of 0.0004%, just before use. After 20 min in the staining solution, the slides were rinsed for one min in each of three distilled water washes. The slides were then placed on a slide warmer, set at approximately 50^0C, until they were fully dry. The dry slides were cleared by immersion in xylene for at least a min before cover-slipping with DPX (Fluka, Milwaukee WI, USA; or Sigma Chem. Co., St. Louis MO, USA), a non-aqueous, non-fluorescent plastic mounting media, followed by thorough examination.

Additional sections were immunostained for the detection of phosphorylated tau- related pathology and astrogliosis. Briefly, sections were rinsed in tris-buffered solution and following incubation with a blocking buffer, were treated with primary antibodies against phosphophorylated tau (AT-8, AT180; Innogenetics) or glial fibrillary acidic protein (GFAP; DakoCytomation, Denmark). AT8 and AT180 immunoreactivities were then visualized with a modified labeled streptavidin (LSAB) technique (Dako LSAB2 System Peroxidase), whereas for glial fibrillary acidic protein (GFAP), incubation with goat anti-rabbit (Vector, Burligame, CA, USA) secondary antibody followed by avidin – biotin complex treatment, was performed. The peroxidase reaction was visualized with 0.05% 3.3'-diaminobenzidine (DAB) and 0.02% hydrogen peroxide. Sections were then counterstained with hematoxylin, dehydraded in ethanol and cleared in xylene. In a number of sections, double immunohistochemistry for either AT8 or AT180 and GFAP, was performed. In these cases, the first and the second primary antibody reactions were visualized with DAB and VIP (Vector Laboratories, Burlingame, CA, USA) as chromogens. Omission of the primary antibody was used for negative controls.

Quantitative assessment of neurodegeneration and astrogliosis. In each group (ADNP+/+ and ADNP+/- male mice), the numbers of Fluoro-Jade-stained neurons in cortex and

hippocampus, of both hemispheres, were determined as described (Sato et al., 2001) with some modifications. Analysis was performed on three adjacent sagittal sections obtained at the 5 brain levels. Fluoro-Jade-positive neurons were quantified by capturing the images from a number of visual fields in each section onto an Intel Pentium computer using a digital camera (NIKON DS-5Mc-L1) mounted on a microscope. In the cortex, 8-10 randomly selected visual fields were captured and the final magnification of the captured images was X240. A square, 610X610 µm with 100 square subdivisions (6.1 X 6.1 µm), was centered in each captured image. In the hippocampus, images of CA1, CA3, CA4 and hillus areas were captured along the whole hippocampal area with a final magnification of X480. Depending on the size of each area, 2-4 images were captured. In each image, a rectangle, 305X122 µm with 40 square subdivisions (3.05 X 3.05 µm) was positioned over the captured hippocampal area.

For all captured images, each square subdivision was counted if it contained at least one labeled element, defined as a labeled cell body and/or its processes. The tissue section, which exhibited the greatest number of Fluoro-Jade-positive structures, was selected for statistical analysis (Sato et al., 2001). The scores of the areas studied represented subjective assessments of fluorescence intensity and numbers of labeled cells, as follows: In the cortex: 0: no labeling observed in any square subdivision; 1 (+): 1-10 square subdivisions positive; 2 (++): 11-30 square subdivisions positive; 3 (+++): 31-60 square subdivisions positive; 4 (++++): >60 square subdivisions positive. In the hippocampus: 0: no labeling observed in any square subdivision; 1 (+): 1-10 square subdivisions positive; 2 (++): 11-20 square subdivisions positive; 3 (+++): >20 square subdivisions positive.

The number of AT8 and AT180 positive glial cells were assessed semi-quantitatively using light microscopy, in 3 serial sections adjacent to those selected for Fluoro-Jade B

evaluation at all 5 pre-selected brain levels. A total of 8 randomly selected microscopic fields per section, each of 22500 μm^2 as defined by an ocular morphometric grid adjusted at the prefrontal lens, were evaluated. The scores of the areas studied represented subjective assessments of staining intensity and numbers of labeled cells, as follows: 0: no labeling observed; 1 (+): small number of cells that are only weakly labeled; 2 (++): moderate number of cells that are clearly labeled; 3 (+++): large number of intensely labeled cells present (Simic et al., 2000).

All quantitative assessments were performed by two independent observers. In cases where significant discrepancies were obvious between the two observers, the evaluation was repeated by a third individual.

Statistical Analyses. Statistical tests used one-way ANOVA with pairwise multiple comparison procedures (Student-Newman-Keuls method). Histological and immunohistochemical data used semi-quantitative and non-parametric statistics.

Results

ADNP partial deficiency results in multiple gene expression changes – measurements during pregnancy. To identify downstream target genes of ADNP, global gene expression profiles of whole E9 knockout embryos (KO - ADNP-/-), their wild-type (WT - ADNP+/+) and their heterozygous (H – ADNP+/-) littermates, were examined using the Affymetrix microarrays (Mandel et al., 2007). E9 embryos were chosen because it is the period by which embryos lacking ADNP exhibit distinct morphological and developmental changes just prior to degeneration and in utero absorption (Mandel et al., 2007). In contrast to ADNP-/- embryos, the heterozygous embryos undergo normal embryogenesis, albeit with slight developmental delays, exhibiting viable phenotype (Pinhasov et al., 2003). Similarly, complete ADNP deficiency results in major changes in gene expression (Mandel et al., 2007). Here, the heterozygous phenotype exhibited minor changes in gene expression including upregulation in a number of central gene products (Fig. 1A). These upregulated genes are involved in key cellular functions including transcription, nervous system development, and control of DNA and dopamine metabolism as well as signaling pathways (Fig. 1B). These results suggested potential global effects for ADNP on mature brain activity, which may be deciphered with ADNP+/- mice.

To further validate the array data and to identify potential changes in adult ADNP+/- mice, we chose to follow-up the expression of Pax6, a gene that showed increased expression in the ADNP+/- embryos (Fig. 1A,B) and that was found to be expressed in the adult subcortical domains (Stoykova and Gruss, 1994). Quantitative reverse transcription and real time PCR was performed on individual RNA samples prepared from subcortical domains of two-months-old male mice (ADNP+/+, n=4; ADNP+/-; n=4, each in triplicates). Results showed a significant 2.104$\pm$0.267 -fold increase in Pax6 expression in the ADNP+/- mice (p<0.004).

JPET Fast Forward. Published on August 24, 2007 as DOI: 10.1124/jpet.107.129551
This article has not been copyedited and formatted. The final version may differ from this version.

ADNP partial deficiency results in reduced neuroprotective potential – measurements in newborn brains. Given the changes in gene expression that were observed above, the finding of ADNP as a glial protein (Bassan et al., 1999; Furman et al., 2004) and the neuroprotective activity of recombinant ADNP (Steingart and Gozes, 2006), it was of interest to evaluate the degree of protective support given by an astrocyte feeder layer derived from ADNP+/- mice to neuronal cultures. Astrocytes were derived from newborn cerebral cortical tissues. Results showed a significant reduction in neuronal survival from 410 $\pm$ 22 neurons in the ADNP+/+ cultures to 334 $\pm$ 20 in ADNP+/- supported cultures. (n= 4 independent experiments, each in triplicates; $p<0.01$).

Reduced ADNP expression in the brains of 2 month old ADNP+/- mice. Quantitative reverse transcription real time PCR (QRT-PCR) was utilized to analyze ADNP expression (Fig. 2A). QRT-PCR was performed on mRNA isolated from two-month-old male mice tissues. A reduction of 42% in the cortex, of 38% in cerebellum and of 50% in hippocampus was observed in the levels of ADNP mRNA in ADNP+/- male mice as compared to ADNP+/+ mice (Fig. 2A). Northern blot hybridization (Bassan et al., 1999; Zamostiano et al., 2001) indicated similar results (not shown).

At the protein level, ADNP expression was assessed by western analysis (Furman et al., 2004) using actin as a control. As expected, results showed reduced expression of ADNP at the protein level in ADNP+/- mice at all ages tested. An example for nine-month-old mice (cerebral cortex tissue) is shown for both control (densitometric scanning results in comparison to actin standardized at 100%, 100$\pm$24, n=3) and ADNP+/- (34.7$\pm$3, n=3), $p<0.01$; (Fig. 2B).

Phosphorylated tau is increased in the brains of ADNP+/- mice, and is reduced by NAP treatment. As shown above, ADNP-deficiency was associated with multiple changes in

JPET Fast Forward. Published on August 24, 2007 as DOI: 10.1124/jpet.107.129551
This article has not been copyedited and formatted. The final version may differ from this version.

gene expression and reduced neuronal survival. Thus, tau phosphorylation (a major marker for neurodegeneration) was investigated in the cerebral cortex of the ADNP-deficient male mice in comparison to control mice (ADNP+/+). Two antibodies [AT-8 and AT180] that recognize different sites of phosphorylation on tau, (Ser202/Thr205) and (Thr 231), respectively, were used and results were calibrated against actin immunoreactivity as an internal standard. Two age groups were tested, two-month-old mice and nine month-old mice. The two-month-old mice were further divided into two groups, one injected daily with saline (subcutaneous), for the first two weeks of life and one similarly injected with NAP. Densitometric analysis of the Western blots at two months of age (Fig. 3A) showed a ~40% increase in tau phosphorylation (Ser202/Thr205) in the ADNP+/- mice as compared to the ADNP+/+ mice ($p<0.05$). Daily injection of NAP for the first two weeks of life resulted in >2-fold reduction in tau phosphorylation (Ser202/Thr205) in the ADNP+/- mice ($p<0.001$) (Fig. 3A). The increase in tau phosphorylation in ADNP+/- mice as compared to ADNP+/+ mice and the decrease after NAP treatment were also apparent when the results were calibrated against total tau immunoreactivity (tau5 antibody; $p<0.01$) (Fig. 3A).

Since phosphorylated tau increased in the cortex of ADNP+/- mice, the levels of the active [phosphor-GSK3α/β (pTyr279/216)] and the inactive [GSK3β(pSer9)] forms of GSK3, which regulate phosphorylation at specific sites of tau, were measured in the protein extracted from the cerebral cortex of two-months-old male mice. While there was only a small, statistically insignificant increase in the ratio of active/inactive GSK3βin ADNP+/- mice as compared to ADNP+/+ mice, NAP treatment resulted in a significant ($p<0.05$) ~2-fold reduction in the ratio of active/inactive GSK3βin both ADNP+/- and ADNP+/+ mice (Fig. 3A).

JPET Fast Forward. Published on August 24, 2007 as DOI: 10.1124/jpet.107.129551
This article has not been copyedited and formatted. The final version may differ from this version.

The increased tau phosphorylation in ADNP+/- mice as compared to ADNP+/+ mice was maintained as the mice matured, as seen at nine months of age (Fig. 3B). Similar results were obtained for both phosphorylation at (Ser202/Thr205) and (Thr 231) on tau. In comparison to the insignificant increase in the ratio of active/inactive GSK3β in two-month-old ADNP+/- mice, the older, nine-month-old mice showed a significant 50% increase in active GSK3β, as shown in the ratio of active/inactive enzyme (Fig. 3B, $p<0.01$).

Neurodegeneration and the appearance of astrocytic tau-like pathology in ADNP+/- mice. Male mice (5-11-month-old) were analyzed for potential tau pathology at the anatomical level. Double labeling with phosphorylated tau antibodies and antibodies to glial fibrillary acidic protein (GFAP), for specific astrocyte staining were conducted. Results showed that among the ADNP +/- male mice there was a high prevalence of "thorn-shaped" astrocytes. Tau-related pathology was evident both in the soma and in the processes in a number of swollen astrocytes as well as in numerous isolated thread-like processes (Fig. 4 A-D, A,C, ADNP+/+; B,D, ADNP+/-) in the 11-month-old ADNP+/- mice. In addition, the number of swollen astrocytes, regardless of whether they presented tau-related pathology or not, was higher in 10-11-month-old ADNP+/- male mice when compared to age-matched ADNP+/+ animals. GFAP/AT8 or AT180-labeled astrocytes did not show significant differences (not shown). Accordingly, GFAP/AT8 or AT180-labeled astrocytes with varying morphologies were counted and results indicated that dystrophic astrocytes exhibiting tau-related pathology were found at significantly higher percentage in the ADNP+/- animals as compared to ADNP+/+ mice. Comparative analysis, performed according to the scale described in the materials and methods section, showed that the vast majority (% of visual fields) with normal appearing astrocytes (grade 0) were higher among the ADNP+/+ compared to ADNP+/- male mice. In contrast, a higher number of grades 1, 2 and

3 dystrophic astrocytes were found in the brain of ADNP+/- animals as compared to ADNP+/- mice (Fig. 4E, $p<0.001$). The distribution of astrocytes was not specific; thorn- or tuft- like astrocytes were located at the parahippocampal area, thalamus, cerebellum and brainstem. The age of onset for such an astroglial reaction was > eight months, since at this age, a less intense staining either for AT8 or AT180 was detected in the ADNP+/- mice when compared to eleven-months-old ADNP+/- male mice.

The tau immunohistochemistry results that indicated neurodegeneration and astrocyte damage were corroborated by Fluoro-Jade B staining in both the hippocampus and the cortex of the ADNP+/- mice (Fig. 5A-H, A,C,E,G, ADNP+/+; B,D,F,H, ADNP+/-). Neurodegeneration increased with age and was most apparent at eleven months of age. Comparative analysis showed that the vast majority (% of visual fields) with normal appearing neurons (grade 0) were higher among the ADNP+/+ compared to ADNP+/- male mice. In contrast, a higher number of grades 1, 2 and 3 dystrophic neurons were found in the cortex of ADNP+/- animals as compared to ADNP+/- mice ($p<0.001$, Fig. 5I). Similar results were found in the hippocampus (Fig. 5J, $p<0.001$). Degenerative neurons were not evident before the eighth month of age.

ADNP+/- mice exhibit significant spatial learning deficits. Three different studies were performed to assess potential spatial learning and memory deficits under the influence of the ADNP-deficient phenotype and possible reversal by the ADNP-derived neuroprotective peptide, NAP (Gozes et al., 2005a). In the first study, two month old ADNP+/- male mice were treated by intranasal administration of either vehicle or NAP (daily treatments for 2 weeks) and those were compared to vehicle-treated ADNP+/+ male mice. In the second study, newborn mice were injected (subcutaneous) daily for two weeks with increasing concentrations of NAP or vehicle (Bassan et al., 1999). The third study, included mice treated as in the second studies that

were further subjected to NAP or vehicle treatment (daily intranasal administration) at the age of nine months for two weeks. The first two groups were subjected to a Morris water maze at the age of nine weeks. The nine-month-old mice were subjected to the Morris water maze at nine months plus a week. Groups 1 and 3 continued to receive NAP during the 5-testing days of the water maze.

Behavioral assessments were performed in a water maze by measurements of the time required to find a hidden platform. Two daily tests were performed over five testing days. The platform location and the animal's starting point were held constant within each pair of daily trials, but the location of the platform and the animal's starting point were changed every day (Gozes et al., 2000). In the first daily test, indicative of reference memory, ADNP+/- male mice were impaired compared to control animals (*$p < 0.05$, **$p < 0.01$, ***$p < 0.001$; Fig. 6 A,C,E). Furthermore, while the two month old ADNP+/+ mice learned the task after 3 testing days (#$p < 0.05$, ##$p < 0.01$, ###$p < 0.001$), ADNP+/- male mice did not learn the task (Fig. 6 A,B). At nine months of age, the ADNP+/+ did not show significant improvement in the latency to find the hidden platform in a water maze over a five day testing period (Fig. 6E). However, significant differences were apparent between the ADNP+/+ mice, the ADNP+/- mice, with the ADNP+/- mice exhibiting increased latencies to find the hidden platform (Fig. 6E). NAP treatment significantly improved water maze performance as evidenced in studies 1 and 3 on the fifth testing day (Fig. 6A, Fig. 6E). In study 2, NAP treatment significantly improved learning on the third day that was not apparent in the vehicle-treated ADNP+/- mice (Fig. 6C).

In the second daily test, that evaluates short-term working memory, significant differences between ADNP+/- and ADNP+/+ male mice were apparent between the second and fifth days of testing, depending on the study group ($p < 0.05$, Fig. 6B,D,F). In contrast to the

ADNP+/+ mice that learned the task, no significant learning curve was observed in the ADNP+/- male mice at nine months of age (**$p < 0.01$, Fig. 6F). Similar results in the Morris water maze were obtained with 2-month-old mice that showed learning impairment (Fig. 6B,D). NAP treatment significantly improved water maze performance as evidenced in studies 1 and 3 on the fifth testing day (Fig. 6B, Fig. 6F). NAP treatment was also assessed in ADNP+/+ mice showing minor changed at two months of age and significant improvement at nine months of age as shown before [data not shown, (Alcalay et al., 2004)]. On the last testing day, the mice were subjected to a visible platform test to assess their motor abilities. All tested mice found the visible platform over a 60 second test period. The mean platform finding time was 11.52 $\pm$ 1.65 sec (n=21, two month old ADNP+/+ males, receiving saline for the first two weeks of life), 22.42 $\pm$ 5.39 (n=14; two month old ADNP+/- males, receiving saline for the first two weeks of life) and 26.3 $\pm$ 8.3, (n=10; two month old ADNP+/- males, receiving NAP for the first two weeks of life), suggesting a significant difference between the ADNP+/- and the ADNP+/+ group at 2 months of age ($p<0.05$), which was not ameliorated by NAP treatment. However, at 9 months of age with two weeks NAP or vehicle nasal treatment, no significant differences were observed and the mean platform finding time was 24.00 $\pm$ 9.58 sec (n=8, ADNP+/+ males) and 26.6 $\pm$ 10.47 (n=5; ADNP+/- males) and 11.17 $\pm$ 4.6, (n=6; NAP-treated ADNP+/- males). An additional test for motor performance was the open field test. Here also, no differences were observed between ADNP+/- and ADNP+/+ male mice (even when the test period was extended from 3 minutes to one hour, data not shown), however, a statistically significant difference was found between two-month-old mice and nine-month-old mice, suggesting an age-dependent reduction in motor activity (Fig. 6G).

To strengthen the results regarding potentially reduced memory capabilities in the ADNP+/- mice, a social recognition test was implemented. Olfactory cues are the predominant mechanism through which social familiarity develops (Hill et al., 2007) and results depicted in Fig. 6H showed that 1] ADNP+/- mice significantly differed from control, ADNP+/- mice, in their recognition of novel females (both female 1 and female 2; $p<0.05$). 2] While both ADNP+/- and ADNP+/+ mice habituated to the novel mouse and sniffed and followed the female less with succeeding introductions through trials 1 through 5, the habituation was more rapid for the ADNP+/+ mice showing a significant reduction already during the second trial with the female 1 ($p<0.01$), while the ADNP+/- mice were slower and showed significant reduction in sniffing and following female 1 only on the third trial ($p<0.05$ as compared to the first trial with female 1). 3] Furthermore, the ADNP+/- mice exhibited an abnormal social memory response because, unlike control mice, they did not show renewed interest with the introduction of an unfamiliar female in trial 6. While the ADNP+/+ mice sniffed and followed the novel female significantly longer in trial 6 as compared to trial 5 ($p<0.01$), there was no significant increase in the ADNP+/- mice.

Discussion

The current study showed that ADNP+/- mice exhibited reduced expression (~50%) of brain ADNP and an increase in markers of neuronal degeneration that are associated, in part, with tauopathy. Furthermore, a decreased ability of the ADNP-deficient astrocytes to support neuronal survival was observed. Motor activity was similar in the ADNP+/- male mice as compared to ADNP+/+ male mice. In contrast, learning deficits in the Morris water maze were apparent at two months and were sustained at nine months of age in ADNP+/- male mice. These results were corroborated in a social interaction working memory test with three-month-old male mice. Treatment with the ADNP-derived neuroprotective peptide NAP resulted in reduced tau hyperphosphorylation and increased performance in the Morris water maze that evaluates spatial learning and memory.

Studies in other laboratories indicated that deletions in the human ADNP chromosomal region [20q12–13.2, (Zamostiano et al., 2001)] may be associated with mental retardation in man (Borozdin et al., 2007). Most recently, a reduction in the ADNP mRNA levels was observed in the cerebral cortex and astrocytes from prenatal ethanol exposed (PEE) rat fetuses. Furthermore, co-cultures of PEE astrocytes with control neurons caused a marked decrease in neuronal growth, differentiation and synaptic connections relative to the co-cultures with control astrocytes, effects that were reverted by the addition of NAP (Pascual and Guerri, 2007). Other studies showed that prenatal NAP administration, in combination with ADNF-9 (SALLRSIPA), prevented the alcohol-induced spatial learning deficits and attenuated alcohol-induced proinflammatory cytokine increase in a model of fetal alcohol syndrome (Vink et al., 2005).

Decreased ADNP content was associated with changes in the expression of several gene products (Fig. 1A,B) including Pax6. Our results indicate a complex association between Pax6 and ADNP expression, as complete ADNP knockout resulted in a significant reduction in Pax6 expression in the primordial brain area (Pinhasov et al., 2003), while here, a partial deficiency in ADNP resulted in increases in Pax6 in the developing embryos as well as in subcortical domains of the adult brain. Pax6 has been associated in the specification of the subcortical domains of the evolutionary old limbic system (Stoykova and Gruss, 1994) and in neurogenesis in general. Increases in Pax6 expression may suggest aberrant developmental processes and potential compensatory mechanisms associated with ADNP deficiencies.

Recent findings have shown that ADNP may co-localize with microtubules in the cytoplasm of astrocytes (Furman et al., 2004). The tubulin cytoskeleton is intimately associated with neuronal structure and function [e.g.(Gozes and Sweadner, 1981)] and the pathology of tau, a microtubule-associated protein that loses proper functionality in the hyperphosphorylated state has been implicated in multiple neurodegenerative diseases related to axonal dysfunction (Mandelkow et al., 2003). Intracellular accumulation of hyperphosphorylated tau as neurofibrillary tangles (NFTs) parallels memory disturbances in Alzheimer's disease (Tolnay and Probst, 1999). Disorders sharing similar pathological insoluble tau deposits, collectively called tauopathies, also include Down's syndrome, corticobasal degeneration, progressive supranuclear palsy, Pick's disease, Guam amyotrophic lateral sclerosis/Parkinson's dementia complex and frontotemporal dementia with Parkinsonism chromosome 17- type. Furthermore, tau hyperphosphorylation has been observed in models of diabetes and suggested to contribute to the increased susceptibility to Alzheimer's disease that is observed in diabetic patients (Clodfelder-Miller et al., 2006).

Tau aggregates may be intrinsically toxic, killing neurons directly. Comparative protein analysis of the cerebral cortex of adult ADNP+/- vs. ADNP+/+ mice indicated a significant increase in phosphorylated tau. Furthermore, NAP treatment protected against this increased tau phosphorylation. The target for NAP activity has been suggested to be tubulin, where NAP stimulates microtubule assembly and protects astrocytes (Divinski et al., 2004) and neurons (Divinski et al., 2006) against microtubule dysfunction and tau hyperphosphorylation in cell cultures (Gozes and Divinski, 2004). Recent studies have extended these findings to show that chronic intranasal NAP treatment reduces tau hyperphosphorylation in a mouse model of Alzheimer's disease, the triple transgenic model, that over-expresses both the amyloid beta peptide and hyperphosphorylated tau (Matsuoka et al., 2007).

In the mammalian brain, different kinases, their regulators and phosphatases form multimeric complexes with cytoskeletal proteins and regulate multi-site phosphorylation from synthesis in the cell body to transport and assembly in the axon (Veeranna et al., 2000). Neurodegeneration interferes with the delicate homeostasis resulting in activation of hyperphosphorylation events (Wang et al., 2007). Over-activation of proline-directed kinases, such as cyclin-dependent kinase 5 (Cdk5) and glycogen synthase kinase 3 (GSK3), has been implicated in the aberrant phosphorylation of tau at proline-directed sites (Plattner et al., 2006). While Cdk5 was not implicated in ADNP-deficient pathology (data not shown), the ratio between the active and the inactive forms of GSK3β, was significantly increased in the cerebral cortex of the ADNP+/- male mice (9 months old). It is thus hypothesized that deficits in ADNP will result in decreased astrocyte and neuronal function, leading to increases in active GSK3β toward tau hyperphosphorylation, neurodegeneration and impaired cognition. NAP treatment

that drives microtubules to polymerization and stabilization (Divinski et al., 2004; Divinski et al., 2006) resulted here in normalization of GSK expression.

Morphological evaluations in adult male mice indicated that the ADNP-deficient male mice (>eight months) differ from the corresponding controls, exhibiting increased number of cortical and hippocampal neurons with degenerative features. These morphological changes support the significant spatial learning deficits displayed by the ADNP+/- mice. *In vitro*, astrocytes derived from ADNP+/- mice were already deficient in providing neuronal support at birth. These deficiencies translated into morphological changes at ~ 8 months of age and were more pronounced among the older ADNP+/- animals. ADNP +/- mice exhibited a remarkable astroglial tau-related pathology. AT8 and AT180 – positive material was found to be deposited in a cuff-like manner around astrocytes. In ADNP +/- mice, a number of astrocytes appeared to have either a thorn- or tuft- like shape which may be caused by deposition of intensively labeled AT8- and/or AT180- positive material in the soma and proximal processes. Similar changes have been described in the aged human medial temporal lobe (Grundman et al., 2004). In addition, both the distribution throughout the brain as well as the shape of the affected astrocytes in ADNP+/- mice, share some similarities with the astroglial tau pathology noticed in a number of disorders. In particular, tuft-like astrocytes with tau-related pathology have been reported in progressive supranuclear palsy and tau-positive astrocytic plaques are considered pathognomonic for corticobasal degeneration (Forman et al., 2002; Fulga et al., 2007). Astrocytes play a dynamic role in CNS function, including maintenance of the blood–brain barrier, immune modulation, neurogenesis, synaptogenesis, and modulation of synapse function (Ransom et al., 2003). The astrogliosis observed in tauopathies may be associated with neurofibrillary tangle

formation and not directly astrocytic tau pathology as tau expression in astrocytes is normally low (Togo and Dickson, 2002; Dabir et al., 2006).

Bioinformatic studies map the ADNP gene locus to chromosome 20q13.13-13.2 (Zamostiano et al., 2001) that is flanked by diabetes type II linked genes (Klupa et al., 2000) (http://ensembl.rzpd.de/Homo_sapiens/contigview?c=20:48584983;w=50000.5). For example, the ADNP gene is separated by 3438 base pairs from DPM1 (D20S196; http://www.ncbi.nlm.nih.gov/genome/sts/sts.cgi?uid=57739) that has been linked to diabetes type II (p=0.00010). Diabetes type II has been associated with poor cognitive performance and dementia, particularly in elderly patients. Based on the current results, the ADNP linkage to diabetes might be associated with cognitive outcome in the patients.

In conclusion, this paper describes that functional ADNP is important for neuroprotection *in vivo* through the tau phosphorylation cascade. The ADNP+/- mouse offers a novel paradigm of cognitive deficits associated with tau pathology that may model neurodegeneration related to type II diabetes. Treatment with the drug candidate NAP enhanced cognition and significantly ameliorated deficiencies associated with ADNP knockdown. The significant preclinical promise in NAP is now being tested by Allon Therapeutics with two formulations in Phase II clinical trials in Alzheimer's disease/mild cognitive impairment (AL-108; intranasal), mild cognitive impairment associated with coronary artery bypass graft surgery (AL-208, intravenous) and cognitive impairment associated with schizophrenia (AL-108).

Acknowledgements

We thank Mr. Alexander Kryvoshey for his excellent collaboration on the tissue culture experiments. We thank Drs. Eliezer Giladi and Sharon Furman-Assaf for critical reading of the manuscript. We are grateful to Dr. Douglas E. Brenneman for his invaluable help in the project and Dr. Heiner Westphal for his help in the initiation of this project. Prof. Illana Gozes is the incumbent of the Lily and Avraham Gildor Chair for the Investigation of Growth Factors at Tel Aviv University and the Director of the Adams Super Center for Brain Studies and the Levie-Adersheim-Gitter fMRI Institute. Professor Illana Gozes serves as the chief Scientific Officer of Allon Therapeutics Inc. NAP is in phase II clinical development by Allon Therapeutics Inc.

References

Alcalay RN, Giladi E, Pick CG and Gozes I (2004) Intranasal administration of NAP, a neuroprotective peptide, decreases anxiety-like behavior in aging mice in the elevated plus maze. *Neurosci Lett* **361**:128-131.

Anderson KJ, Miller KM, Fugaccia I and Scheff SW (2005) Regional distribution of fluoro-jade B staining in the hippocampus following traumatic brain injury. *Exp Neurol* **193**:125-130.

Bassan M, Zamostiano R, Davidson A, Pinhasov A, Giladi E, Perl O, Bassan H, Blat C, Gibney G, Glazner G, Brenneman DE and Gozes I (1999) Complete sequence of a novel protein containing a femtomolar-activity-dependent neuroprotective peptide. *J Neurochem* **72**:1283-1293.

Borozdin W, Graham JM, Jr., Bohm D, Bamshad MJ, Spranger S, Burke L, Leipoldt M and Kohlhase J (2007) Multigene deletions on chromosome 20q13.13-q13.2 including SALL4 result in an expanded phenotype of Okihiro syndrome plus developmental delay. *Hum Mutat* **28**:830.

Clodfelder-Miller BJ, Zmijewska AA, Johnson GV and Jope RS (2006) Tau is hyperphosphorylated at multiple sites in mouse brain in vivo after streptozotocin-induced insulin deficiency. *Diabetes* **55**:3320-3325.

Dabir DV, Robinson MB, Swanson E, Zhang B, Trojanowski JQ, Lee VM and Forman MS (2006) Impaired glutamate transport in a mouse model of tau pathology in astrocytes. *J Neurosci* **26**:644-654.

Divinski I, Holtser-Cochav M, Vulih-Schultzman I, Steingart RA and Gozes I (2006) Peptide neuroprotection through specific interaction with brain tubulin. *J Neurochem* **98**:973-984.

Divinski I, Mittelman L and Gozes I (2004) A femtomolar acting octapeptide interacts with tubulin and protects astrocytes against zinc intoxication. *J Biol Chem* **279**:28531-28538.

Forman MS, Zhukareva V, Bergeron C, Chin SS, Grossman M, Clark C, Lee VM and Trojanowski JQ (2002) Signature tau neuropathology in gray and white matter of corticobasal degeneration. *Am J Pathol* **160**:2045-2053.

Fulga TA, Elson-Schwab I, Khurana V, Steinhilb ML, Spires TL, Hyman BT and Feany MB (2007) Abnormal bundling and accumulation of F-actin mediates tau-induced neuronal degeneration in vivo. *Nat Cell Biol* **9**:139-148.

Furman S, Hill JM, Vulih I, Zaltzman R, Hauser JM, Brenneman DE and Gozes I (2005) Sexual dimorphism of activity-dependent neuroprotective protein in the mouse arcuate nucleus. *Neurosci Lett* **373**:73-78.

Furman S, Steingart RA, Mandel S, Hauser JM, Brenneman DE and Gozes I (2004) Subcellular localization and secretion of activity-dependent neuroprotective protein in astrocytes. *Neuron Glia Biology* **1**:193-199.

Gozes I and Divinski I (2004) The femtomolar-acting NAP interacts with microtubules: Novel aspects of astrocyte protection. *J Alzheimers Dis* **6**:S37-41.

Gozes I, Giladi E, Pinhasov A, Bardea A and Brenneman DE (2000) Activity-dependent neurotrophic factor: intranasal administration of femtomolar-acting peptides improve performance in a water maze. *J Pharmacol Exp Ther* **293**:1091-1098.

Gozes I, Morimoto BH, Tiong J, Fox A, Sutherland K, Dangoor D, Holser-Cochav M, Vered K, Newton P, Aisen PS, Matsuoka Y, van Dyck CH and Thal L (2005a) NAP: research and development of a peptide derived from activity-dependent neuroprotective protein (ADNP). *CNS Drug Rev* **11**:353-368.

Gozes I and Sweadner KJ (1981) Multiple tubulin forms are expressed by a single neurone. *Nature* **294**:477-480.

Gozes I, Zaltzman R, Hauser J, Brenneman DE, Shohami E and Hill JM (2005b) The expression of activity-dependent neuroprotective protein (ADNP) is regulated by brain damage and treatment of mice with the ADNP derived peptide, NAP, reduces the severity of traumatic head injury. *Curr Alzheimer Res* **2**:149-153.

Grundman M, Petersen RC, Ferris SH, Thomas RG, Aisen PS, Bennett DA, Foster NL, Jack CR, Jr., Galasko DR, Doody R, Kaye J, Sano M, Mohs R, Gauthier S, Kim HT, Jin S, Schultz AN, Schafer K, Mulnard R, van Dyck CH, Mintzer J, Zamrini EY, Cahn-Weiner D and Thal LJ (2004) Mild cognitive impairment can be distinguished from Alzheimer disease and normal aging for clinical trials. *Arch Neurol* **61**:59-66.

Hill JM, Hauser JM, Sheppard LM, Abebe D, Spivak-Pohis I, Kushnir M, Deitch I and Gozes I (2007) Blockage of VIP during mouse embryogenesis modifies adult behavior and results in permanent changes in brain chemistry. . *J Mol Neurosci* **31**:183-200.

Klupa T, Malecki MT, Pezzolesi M, Ji L, Curtis S, Langefeld CD, Rich SS, Warram JH and Krolewski AS (2000) Further evidence for a susceptibility locus for type 2 diabetes on chromosome 20q13.1-q13.2. *Diabetes* **49**:2212-2216.

Mandel S, Rechavi G and Gozes I (2007) Activity-dependent neuroprotective protein (ADNP) differentially interacts with chromatin to regulate genes essential for embryogenesis. *Dev Biol* **303**:814-824.

Mandelkow EM, Stamer K, Vogel R, Thies E and Mandelkow E (2003) Clogging of axons by tau, inhibition of axonal traffic and starvation of synapses. *Neurobiol Aging* **24**:1079-1085.

Matsuoka Y, Gray AJ, Hirata-Fukae C, Minami SS, Waterhouse EG, Mattson MP, Laferla FM, Gozes I and Aisen PS (2007) Intranasal NAP Administration Reduces Accumulation of Amyloid Peptide and Tau Hyperphosphorylation in a Transgenic Mouse Model of Alzheimer's Disease at Early Pathological Stage. *J Mol Neurosci* **31**:165-170.

Modrego PJ (2006) Predictors of conversion to dementia of probable Alzheimer type in patients with mild cognitive impairment. *Curr Alzheimer Res* **3**:161-170.

Pascual M and Guerri C (2007) The peptide NAP promotes neuronal growth and differentiation through extracellular signal-regulated protein kinase and Akt pathways, and protects neurons co-cultured with astrocytes damaged by ethanol. *J Neurochem*.

Pinhasov A, Mandel S, Torchinsky A, Giladi E, Pittel Z, Goldsweig AM, Servoss SJ, Brenneman DE and Gozes I (2003) Activity-dependent neuroprotective protein: a novel gene essential for brain formation. *Brain Res Dev Brain Res* **144**:83-90.

Plattner F, Angelo M and Giese KP (2006) The roles of cyclin-dependent kinase 5 and glycogen synthase kinase 3 in tau hyperphosphorylation. *J Biol Chem*.

Ransom B, Behar T and Nedergaard M (2003) New roles for astrocytes (stars at last). *Trends Neurosci* **26**:520-522.

Sato M, Chang E, Igarashi T and Noble LJ (2001) Neuronal injury and loss after traumatic brain injury: time course and regional variability. *Brain Res* **917**:45-54.

Simic G, Lucassen PJ, Krsnik Z, Kruslin B, Kostovic I, Winblad B and Bogdanovi (2000) nNOS expression in reactive astrocytes correlates with increased cell death related DNA damage in the hippocampus and entorhinal cortex in Alzheimer's disease. *Exp Neurol* **165**:12-26.

Smith-Swintosky VL, Gozes I, Brenneman DE, D'Andrea MR and Plata-Salaman CR (2005) Activity-Dependent Neurotrophic Factor-9 and NAP Promote Neurite Outgrowth in Rat Hippocampal and Cortical Cultures. *J Mol Neurosci* **25**:225-238.

Steingart RA and Gozes I (2006) Recombinant activity-dependent neuroprotective protein protects cells against oxidative stress. *Mol Cell Endocrinol* **252**:148-153.

Stoykova A and Gruss P (1994) Roles of Pax-genes in developing and adult brain as suggested by expression patterns. *J Neurosci* **14**:1395-1412.

Togo T and Dickson DW (2002) Tau accumulation in astrocytes in progressive supranuclear palsy is a degenerative rather than a reactive process. *Acta Neuropathol (Berl)* **104**:398-402.

Tolnay M and Probst A (1999) REVIEW: tau protein pathology in Alzheimer's disease and related disorders. *Neuropathol Appl Neurobiol* **25**:171-187.

Veeranna, Shetty KT, Takahashi M, Grant P and Pant HC (2000) Cdk5 and MAPK are associated with complexes of cytoskeletal proteins in rat brain. *Brain Res Mol Brain Res* **76**:229-236.

Vink J, Auth J, Abebe DT, Brenneman DE and Spong CY (2005) Novel peptides prevent alcohol-induced spatial learning deficits and proinflammatory cytokine release in a mouse model of fetal alcohol syndrome. *Am J Obstet Gynecol* **193**:825-829.

Wang JZ, Grundke-Iqbal I and Iqbal K (2007) Kinases and phosphatases and tau sites involved in Alzheimer neurofibrillary degeneration. *Eur J Neurosci* **25**:59-68.

Zaltzman R, Alexandrovich A, Beni SM, Trembovler V, Shohami E and Gozes I (2004) Brain injury-dependent expression of activity-dependent neuroprotective protein. *J Mol Neurosci* **24**:181-187.

Zamostiano R, Pinhasov A, Gelber E, Steingart RA, Seroussi E, Giladi E, Bassan M, Wollman Y, Eyre HJ, Mulley JC, Brenneman DE and Gozes I (2001) Cloning and characterization of the human activity-dependent neuroprotective protein. *J Biol Chem* **276**:708-714.

Footnotes:

Unnumbered footnotes:

I. V.S. and A.P. contributed equally to the work in this manuscript

This study was supported, in part, by the U.S.-Israel Binational Science Foundation, the Neufeld Memorial Award, the Israel Science Foundation, Allon Therapeutics, Inc., the Institute for the Study of Aging and the Dr. Diana and Zyga Elton Fund.

This work is in partial fulfillment of the requirements for the Ph.D. degree of Ms. Inna Vulih-Shultzman.

Reprint Requests to: Prof. Illana Gozes, Department of Human Molecular Genetics and Biochemistry, Sackler School of Medicine, Tel Aviv University, Tel Aviv 69978, Israel.

E-mail: igozes@post.tau.ac.il

Legends for Figures:

Figure 1. Patterns of expression in ADNP+/- mice

A. Total RNA from two E9 genotype-identical littermates was used on each Affymetrix array. Two distinct clusters of differential gene expression are shown, for the ADNP+/- and the ADNP+/+ mice (right panel). The Expander clustering program (http://www.cs.tau.ac.il/~rshamir/expander/ver3Help.html#Clustering) was used to graph the homogeneity of the up-regulated and down-regulated gene clusters. Only the up-regulated cluster is shown as the down-regulated was not highly significant.

B. Selected genes that exhibit differential expression in ADNP+/- embryos as compared to ADNP+/+ embryos (see A).

Figure 2. ADNP expression is reduced in ADNP+/- mice

A. ADNP expression in cortex, cerebellum and hippocampus of two-month-old-mice was examined by quantitative real-time PT-PCR. RT-PCR was performed on mRNA isolated from cortex (ADNP+/- n=19; ADNP+/+ n=22), cerebellum (ADNP+/- n=12; ADNP+/+ n=14) and hippocampus (ADNP+/- n=4; ADNP+/+ n=4) of two-month-old ADNP+/- and ADNP+/+ mice. The L-19 ribosomal gene was used as an internal standard.

B. A representative western blot showing an ~50% reduction in ADNP immunoreactivity in ADNP+/- cerebral cortex tissue is shown (n=3 for each group).

Figure 3. Tau phosphorylation is increased in ADNP+/- mice

Western analyses indicating changes in protein expression/phosphorylation in ADNP+/- mice. Protein extracts enriched for tau were prepared from the cerebral cortex of two (**A**) and nine (**B**) -month-old ADNP+/+ and ADNP+/- mice (n=3-5 each).

The blots were probed with specific antibodies against ADNP, phosphorylated tau (AT-8 and AT-180), total tau (TAU 5), GSK-3α/β pY279/216 (active form) and GSK-3β pS9 (inactive form). Actin levels were used to control for the protein loading. The graph represents the densitometric scanning results of the western blots showing mean values of the proteins levels measured in three-five independent experiments, each performed in duplicate. The error bar indicates the standard error. In indicated cases ratios of protein scanning intensities are given (* indicates the difference between ADNP+/+ and ADNP+/- and # indicates the effects of NAP treatment; #,*$p< 0.05$, ##,** $p<0.01$, ###, *** $p< 0.001$).

Figure 4. Tau hyperphosphorylation immunohistochemistry

Double-immunostaining with anti-AT8 (brown) and anti-GFAP (purple) in brain sections of ADNP+/+ (**A**,**C**) and ADNP +/- (**B**, **D**) eleven-month-old male mice. ADNP+/+ exhibited limited astrogliosis (**A**, arrows) compared to ADNP+/- animals (**B**, arrows). AT8 (**D**) depositions co-expressed with GFAP (arrows and arrowheads) either on the cell body which is swollen or the processes of astrocytes, as well as in astroglial threads, were detected only in ADNP+/- animals. Astrocytes may be identified as having either a thorn- (arrows) or tuft- (arrowheads) like shape. The tau-related pathology was evident in astrocytes located at the parahippocampal areas (**B**,**D**) as well as in the thalamus, cerebellum and brainstem (data not shown). (**E**) Seven ADNP+/+ brains and four ADNP+/- brains (eleven-month-old) were subjected to astrocyte counting and

analysis each in 40 different fields. The graph indicate that according to the scale described in the materials and methods section, the vast majority (% of visual fields) with normal appearing astrocytes (grade 0) are among the ADNP+/+ compared to ADNP+/- animals. A number of grade 1 astrocytic pathology is detected in both groups of animals, whereas grade 2 and 3 are only found in ADNP+/- animals.

Figure 5. **Neurodegeneration in ADNP+/- mice**

Degenerative neurons in ADNP+/+ (**A**,**C**,**E**,**G**) and ADNP +/- (**B**,**D**,**F**,**H**) mice are indicated by the Fluoro-Jade B staining. Degenerative neurons (arrows) were evident in the hippocampus of ADNP+/- (CA1 area in **B**) as well as in the cortex (**C**-**H**) of both groups of animals. However, the neurodegenerative changes were minimal in 8-month-old mice (**C**,**D**) and absent at the age of 5 months (**G**,**H**). At the age of 11 months ADNP +/- animals exhibited a significantly higher number of degenerative neurons (**E**,**F,** $p<0.001$). Seven ADNP+/+ brains and four ADNP+/- brains (eleven-month-old) were subjected to neuronal counting and analysis each in 40 different fields. The graphs (**I**, cortical neurons, **J**, hippocampal neurons) indicate that according to the scale described in the materials and methods section, the vast majority (% of visual fields) with normal appearing neurons (grade 0) are among the ADNP+/+ compared to ADNP+/- animals. A number of grade 1 neuronal pathology is detected in both groups of animals, whereas grade 2 and 3 are mostly found in ADNP+/- animals. Statistical evaluation was performed as described in the methods section.

Figure 6. ADNP+/- male mice exhibit spatial learning deficiencies: improvements by NAP treatment: Two daily water maze tests were performed, first (**A,C,E**); second (**B,D,F**). Males

(ADNP+/+, n=5-20; ADNP+/-, n=5-12) were compared. Three different experimental groups were compared. **A,B,** two-month-old mice daily treated by intranasal NAP application for 2 weeks; **C,D,** two-month-old mice daily injected with NAP during the first two weeks of life; **E,F,** nine-month-old mice, daily injected with NAP during the first two weeks of life followed by two weeks of daily intranasal application of NAP at ~ nine months of age. Tests were performed over five consecutive days. **A,C,E** latency measured in seconds (mean $\pm$ S.E.) to reach the hidden platform in its new daily location is depicted. **A,** A significant difference was observed with ADNP+/- compared to ADNP+/+ on training days 3 and 5 (*$p < 0.05$). Significant differences were observed between the first training-day compared to the third through the fifth day of training only in the ADNP+/+ mice (##$p < 0.01$). Intranasal NAP treatment significantly improved performance in the ADNP+/- mice as evident on the fifth testing day (*$p < 0.05$). **C,** A significant difference was observed with ADNP+/- compared to ADNP+/+ on training days 2-5 (*$p < 0.05$). Significant differences were observed between the first training-day compared to the second through the fifth day of training only in the ADNP+/+ mice (###$p < 0.001$). NAP injections significantly improved performance in the ADNP+/- mice as evident on testing days 3-5, indicating learning as compared to the vehicle-treated mice that did not show a learning curve (###$p < 0.001$). **E,** At nine months of age there was no learning curve, however, significant differences were observed on the last (fifth) testing day with ADNP+/+ and NAP-treated ADNP+/- finding the platform significantly faster than the vehicle treated ADNP+/- male mice. **B,D,F,** latency measured in seconds to reach the hidden platform 0.5 min after being on it. **B,** Differences were observed with ADNP+/- compared to ADNP+/+ at the same training day (*$p < 0.05$). Significant differences were observed between the first training-day compared to the third through the fifth day of training only in the ADNP+/+ group (##$p < 0.01$). NAP treatment

significantly improved performance in the ADNP+/- mice as seen on the fifth training day (*p < 0.05). **D,** Differences were observed with ADNP+/- compared to ADNP+/+ at the same training day (**p < 0.01; ***p < 0.001). Significant differences were observed between the first training-day compared to the second through the fifth day of training only in the ADNP+/+ group (###p < 0.001). Some learning was also observed in the ADNP+/- mice and the NAP-treated mouse group. **F,** Differences were observed with ADNP+/- compared to ADNP+/+ at the same training day (**p < 0.01). Significant differences were observed between the first training-day compared to the fourth through the fifth day of training in the ADNP+/+ group (###p < 0.001). NAP treatment significantly improved performance in the ADNP+/- mice as seen on the fourth and fifth training day (##p < 0.01). No differences were observed between the NAP-treated ADNP+/- mice and the vehicle-treated ADNP+/+ mice. **G,** Depicts motor activity in the open field test (path traveled over a three minutes period). No differences were observed between the ADNP+/- and the ADNP+/+ mice at either 2 or 9 months of age. Differences were observed between the two age groups, with nine-month-old mice exhibiting reduced activity (in the two test groups). **H,** Social recognition. Male control (ADNP+/+, n=4) and heterozygote (ADNP+/-, n=3) mice were exposed to aged (18-month-old) female mice for five 5 – min. trials with 30-min. periods of separation between trials. The time the male spent sniffing and following the female was recorded for each trial. On trial 6, a novel female was introduced. *p<0.05, compared to control mice.

Figure 1A

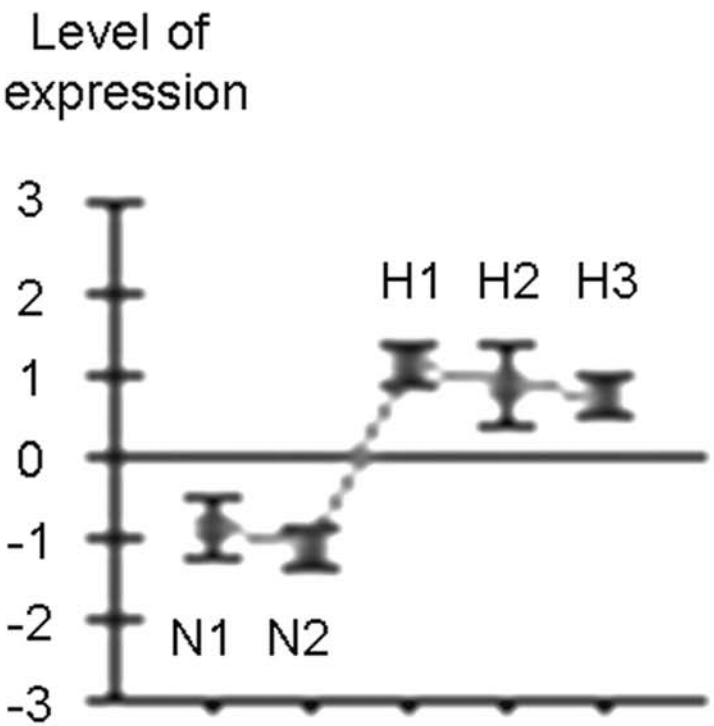

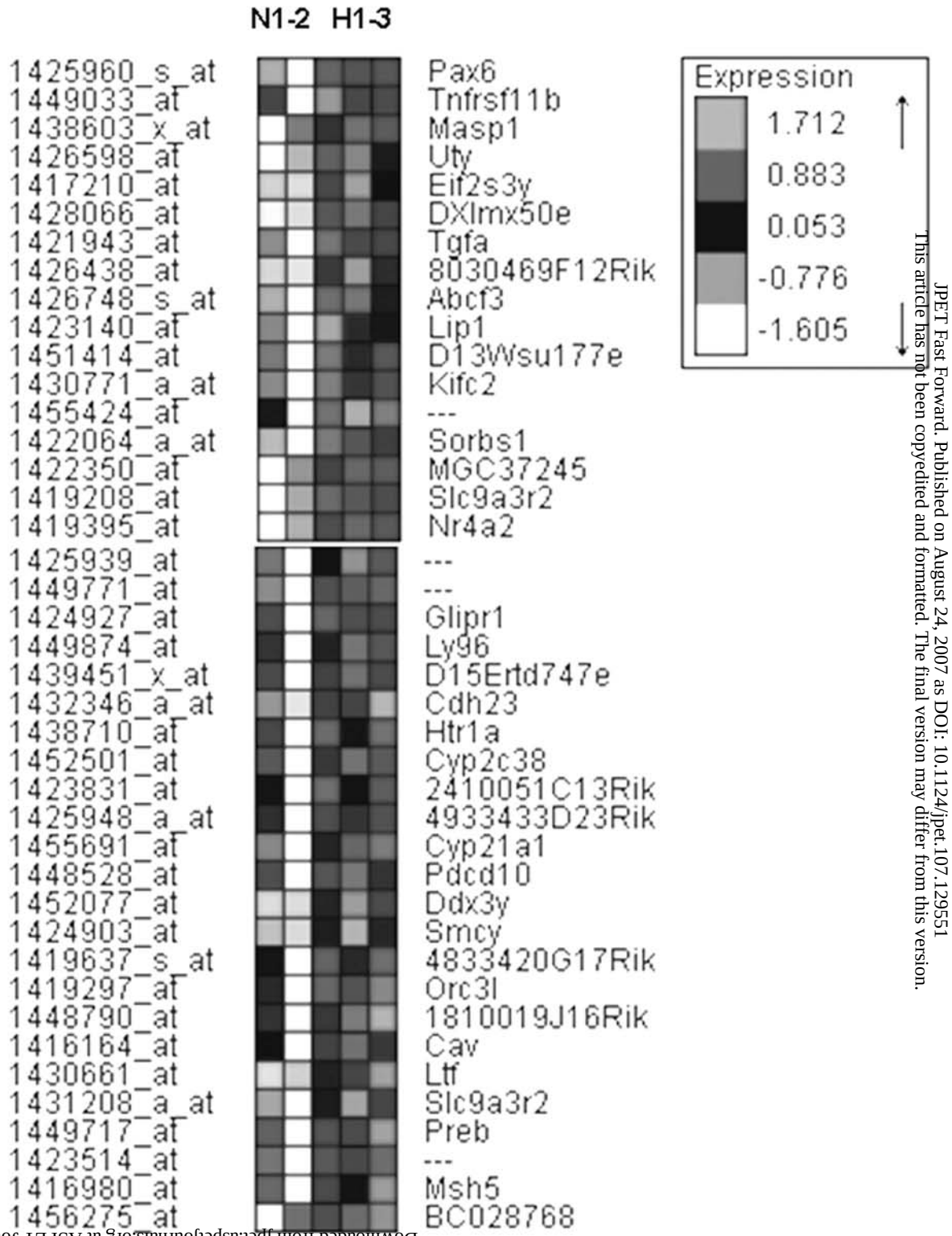

Figure 1B

Selected genes that exhibit differential expression in ADNP+/- embryos as compared to ADNP+/+ embryos

Gene Title	Gene Symbol	GO Biological Process Description	GO Molecular Function Description
Solute carrier family 9	Slc9a3r2	Intracellular signalling cascade	protein binding
Nuclear receptor subfamily 4, group A, member 2	Nr4a2	Transcription, nervous system development, regulation of dopamine metabolism	DNA binding
transforming growth factor alpha	Tgfa	regulation of progression through cell cycle angiogenesis	glycoprotein binding growth factor activity
formyl peptide receptor, related sequence 3	MGC3724 5	G-protein coupled receptor protein signaling pathway	rhodopsin-like receptor activity neuropeptide Y receptor activity purinergic nucleotide receptor activity
lysosomal acid lipase 1	Lip1	lipid metabolism	sterol esterase activity carboxylic ester hydrolase activity
paired box gene 6	Pax6	cell fate determination brain & eye development neuron migration axonogenesis and axon guidance	transcription factor activity
ATP-binding cassette, sub-family F (GCN20), member 3	Abcf3		nucleotide binding ATPase activity nucleoside-triphosphatase activity
mutS homolog 5 (E. coli)	Msh5	DNA metabolism mismatch repair meiosis, female gamete generation DNA metabolism	damaged DNA binding ATP binding
Mannan-binding lectin serine peptidase 1	Masp1	proteolysis immune response complement activation	serine-type endopeptidase activity calcium ion binding sugar binding
tumor necrosis factor receptor superfamily, member 11b (osteoprotegerin)	Tnfrsf11b	apoptosis signal transduction negative regulation of odontogenesis	receptor activity protein binding

JPET Fast Forward. Published on August 24, 2007 as DOI: 10.1124/jpet.107.129551
This article has not been copyedited and formatted. The final version may differ from this version.

Figure 2

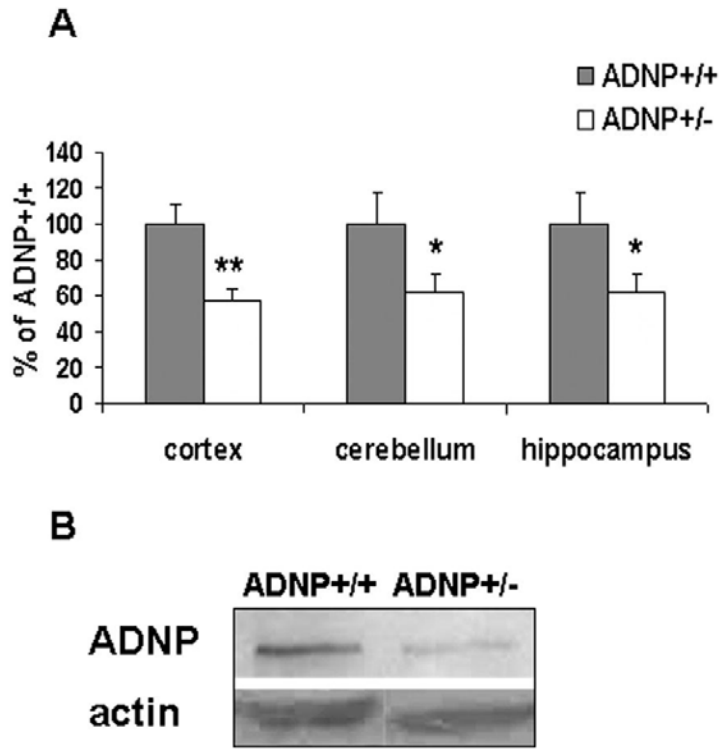

Figure 3A

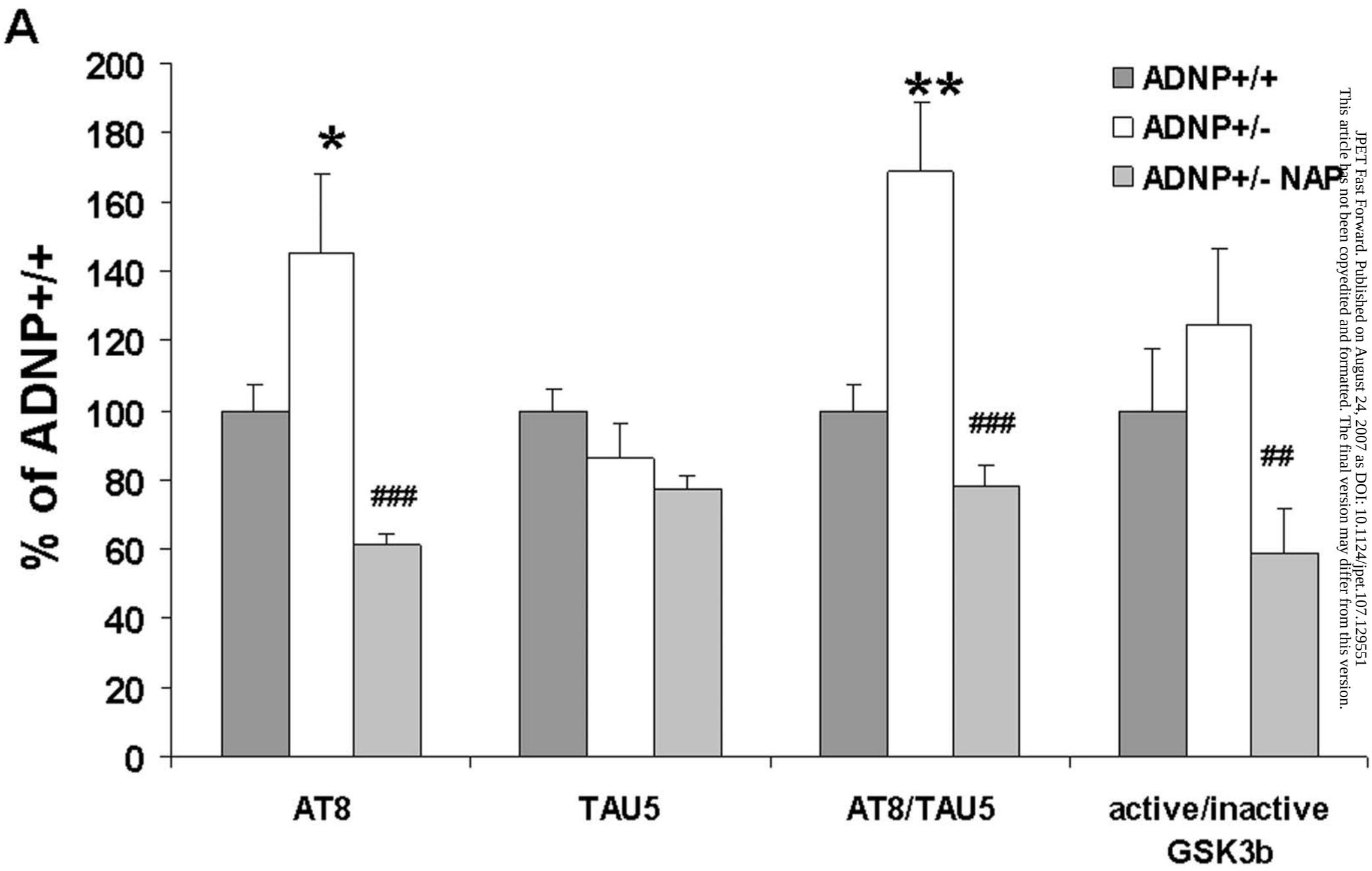

Figure 3B

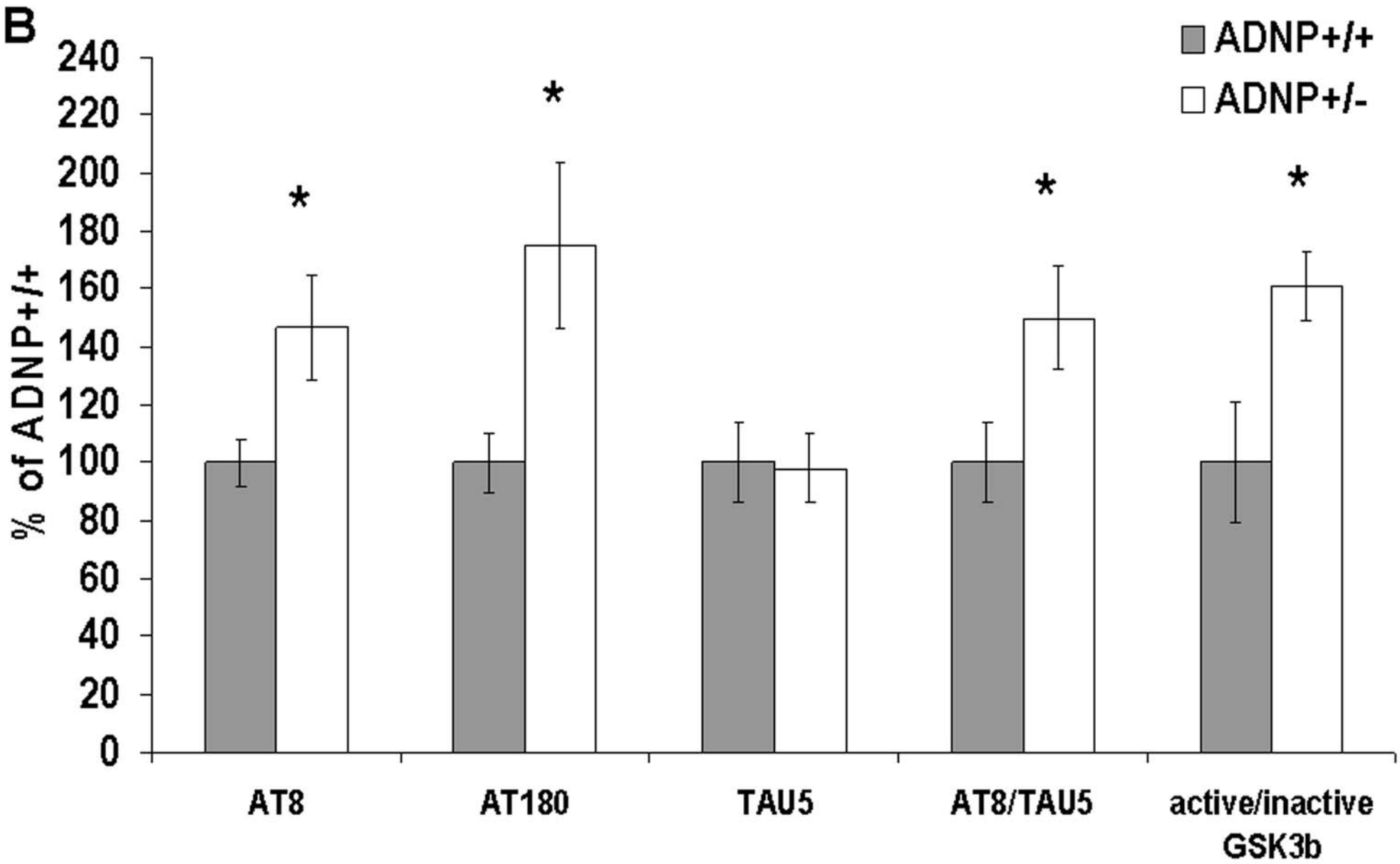

Figure 4, A, B

Figure 4, C,D

Figure 4E

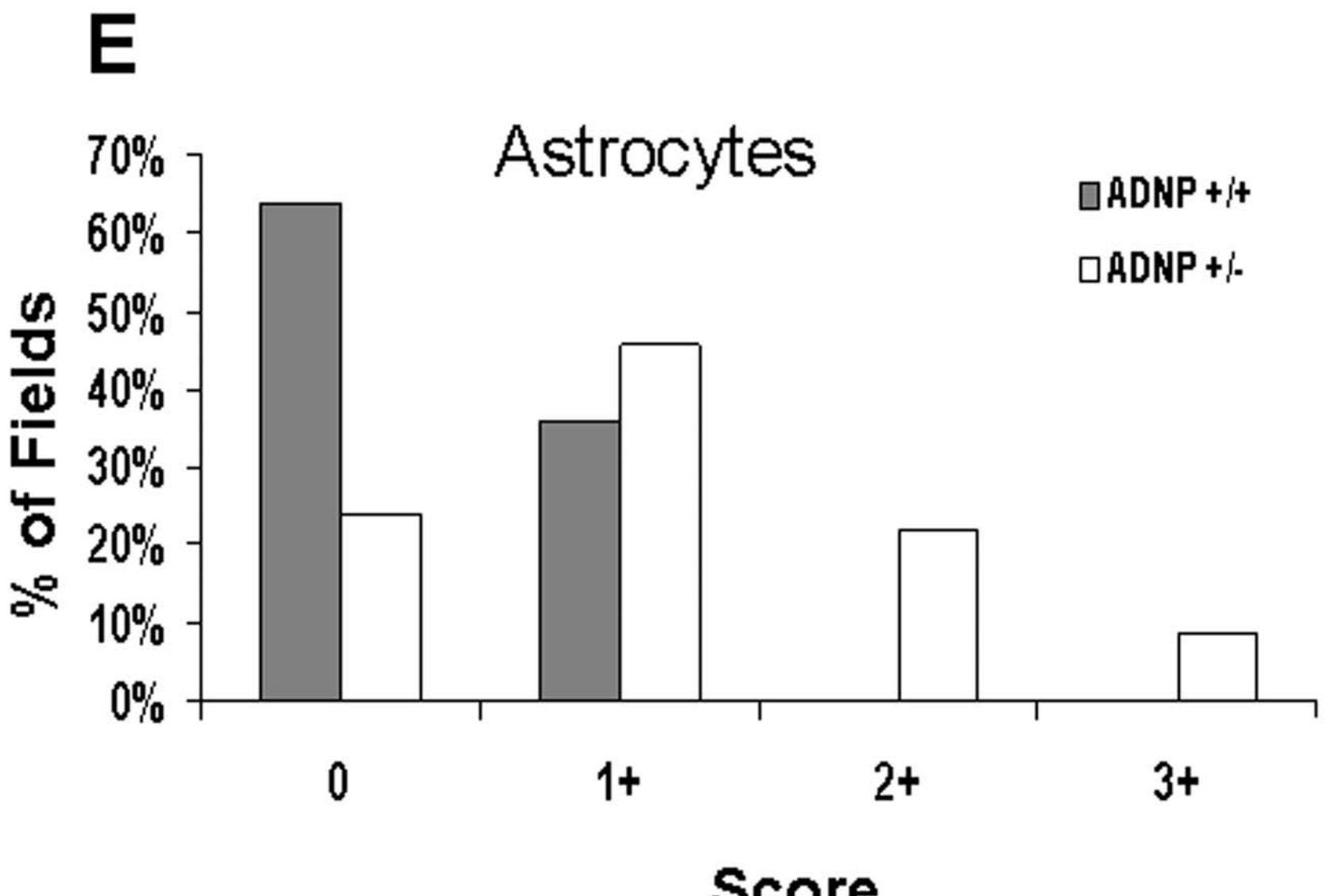

Figure 5, A-D

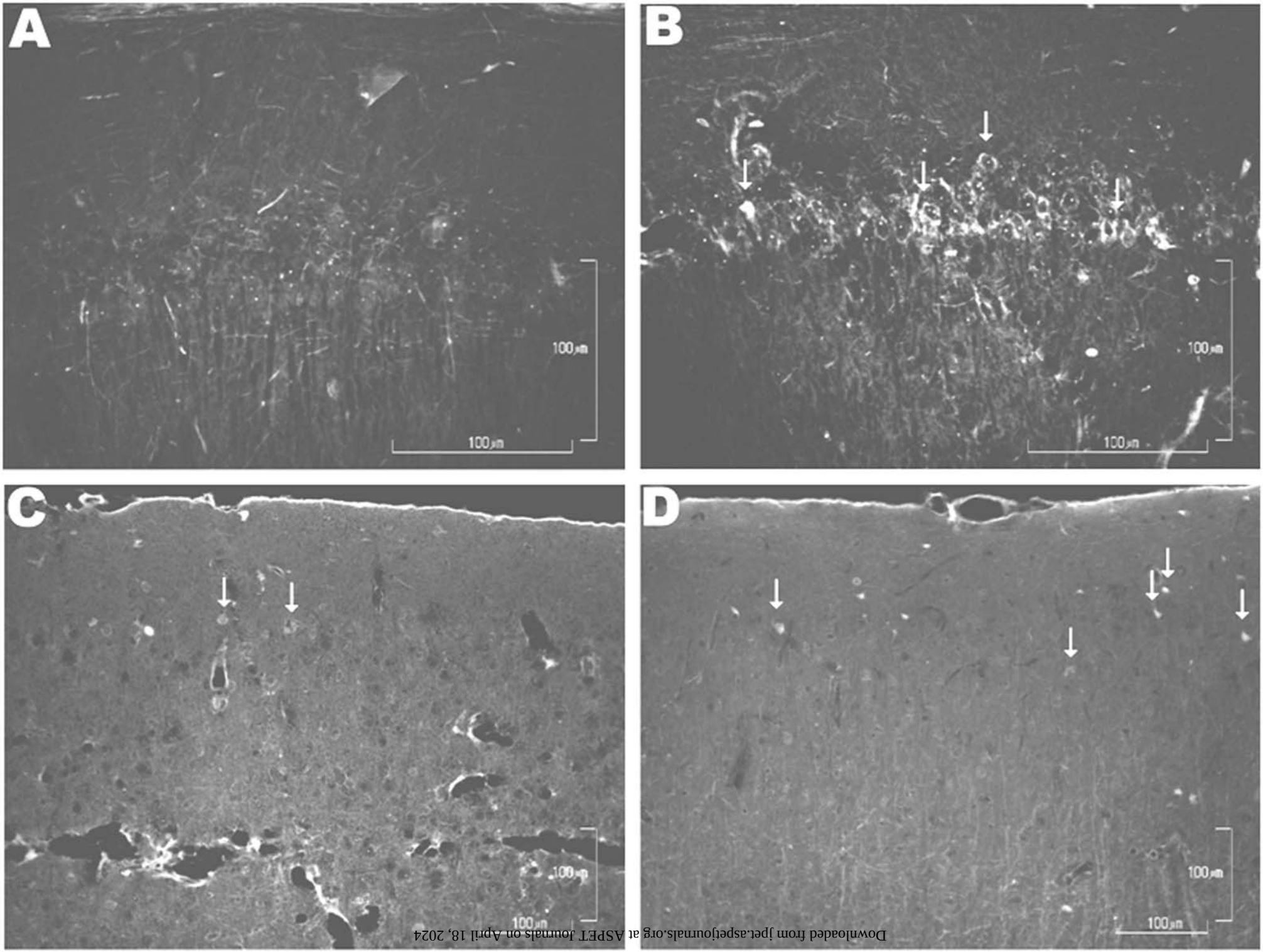

Figure 5, E-H

Figure 5I,J

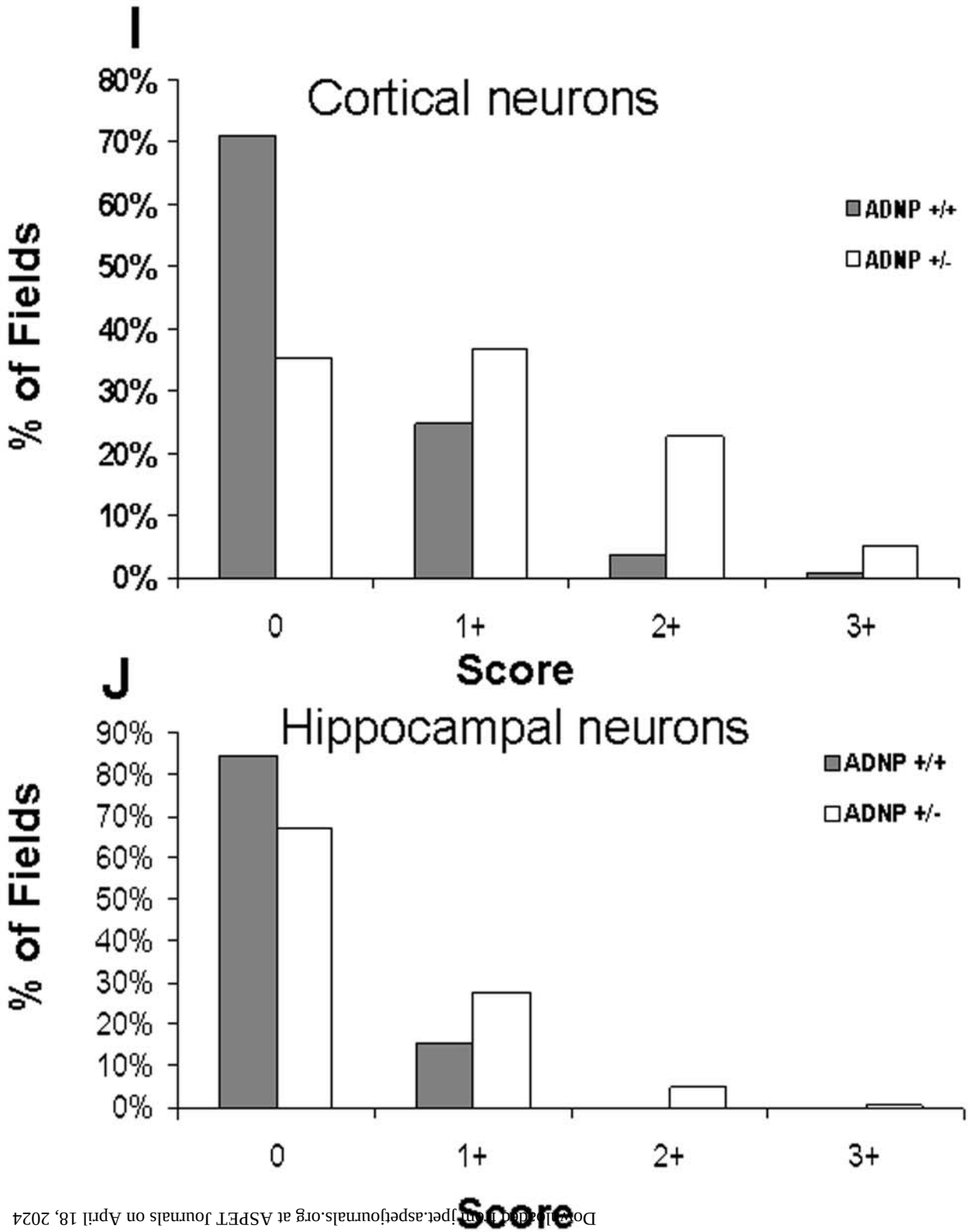

Figure 6A,B

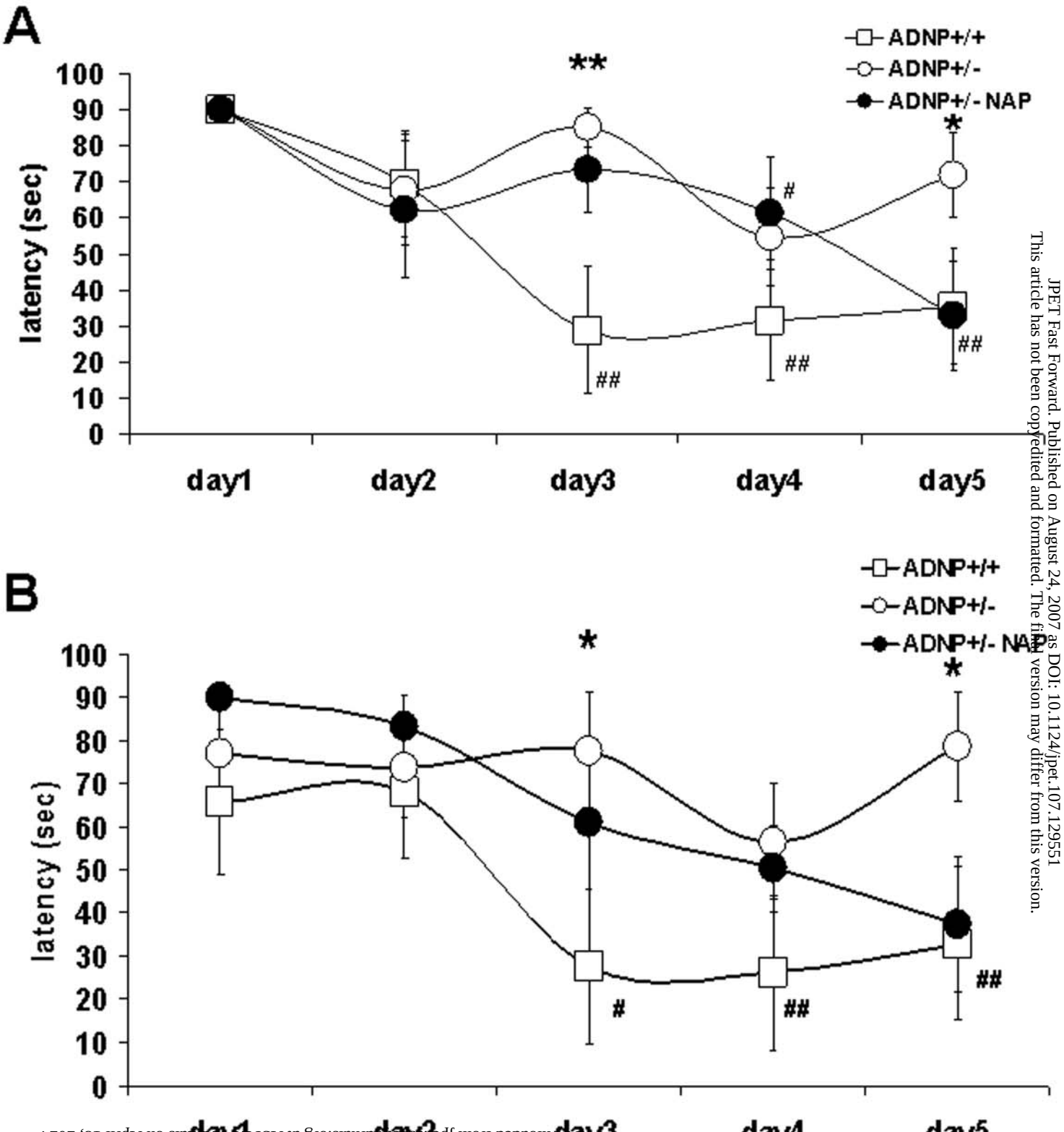

Figure 6C,D

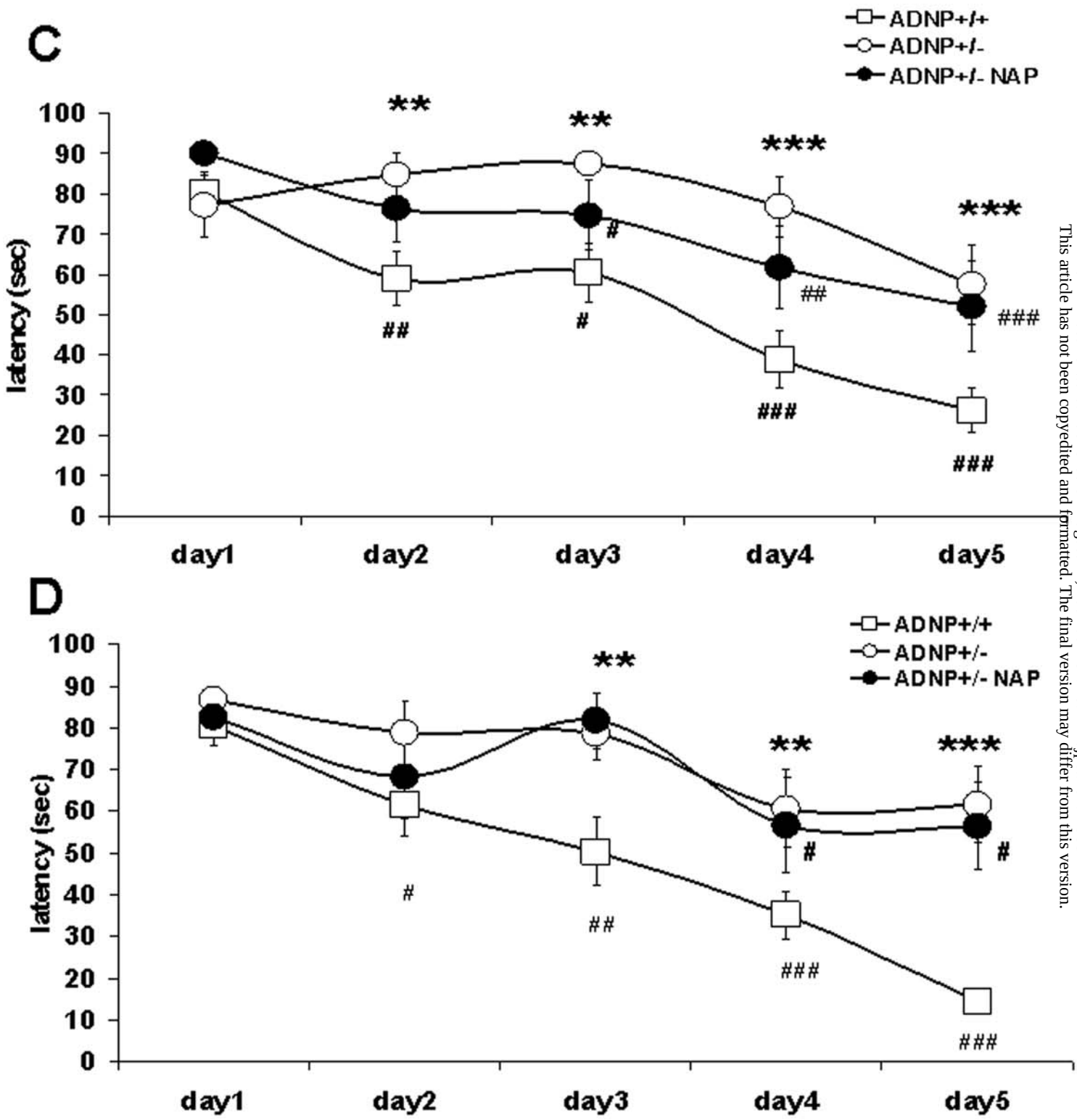

Figure 6E,F

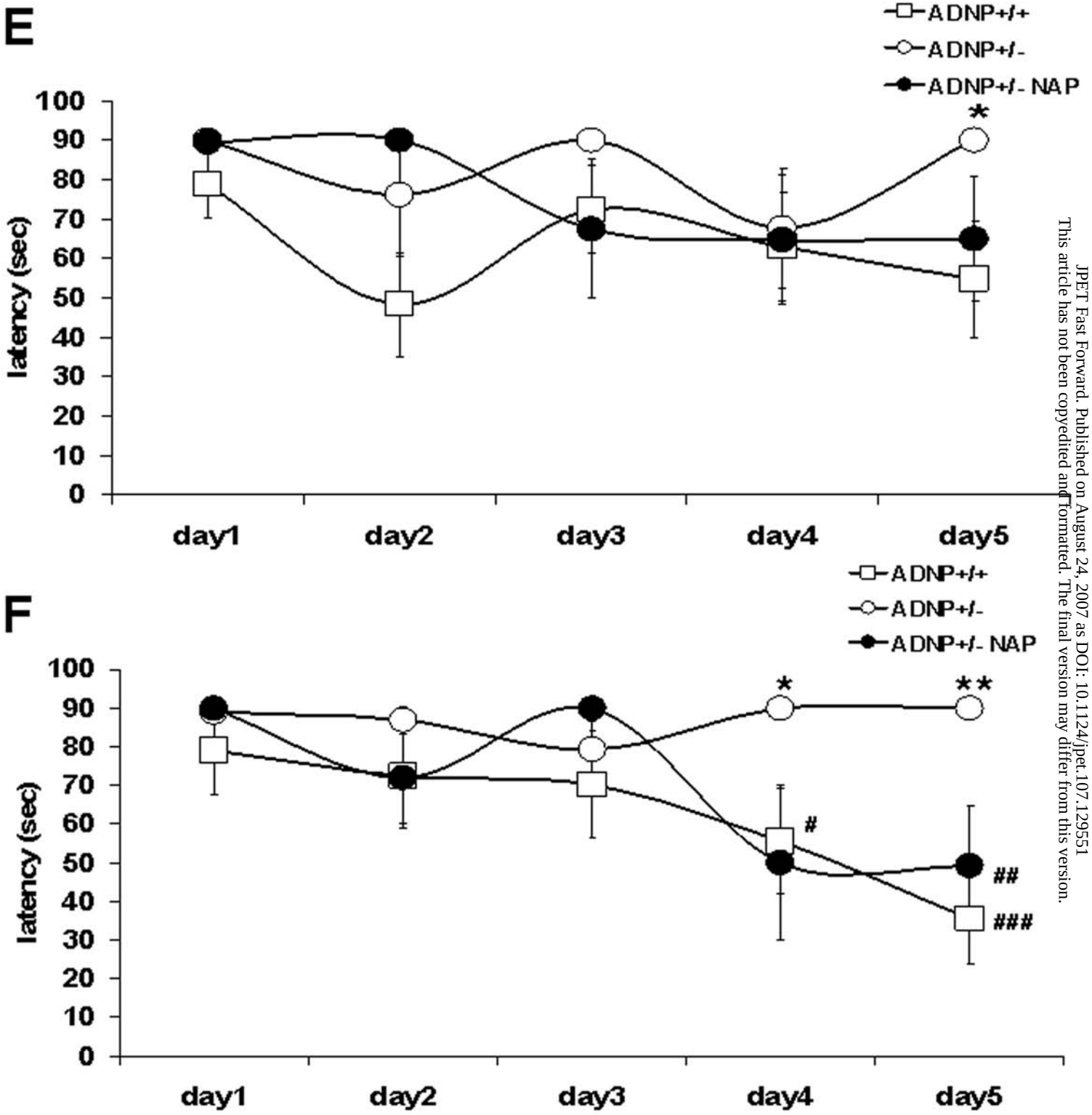

Figure 6G

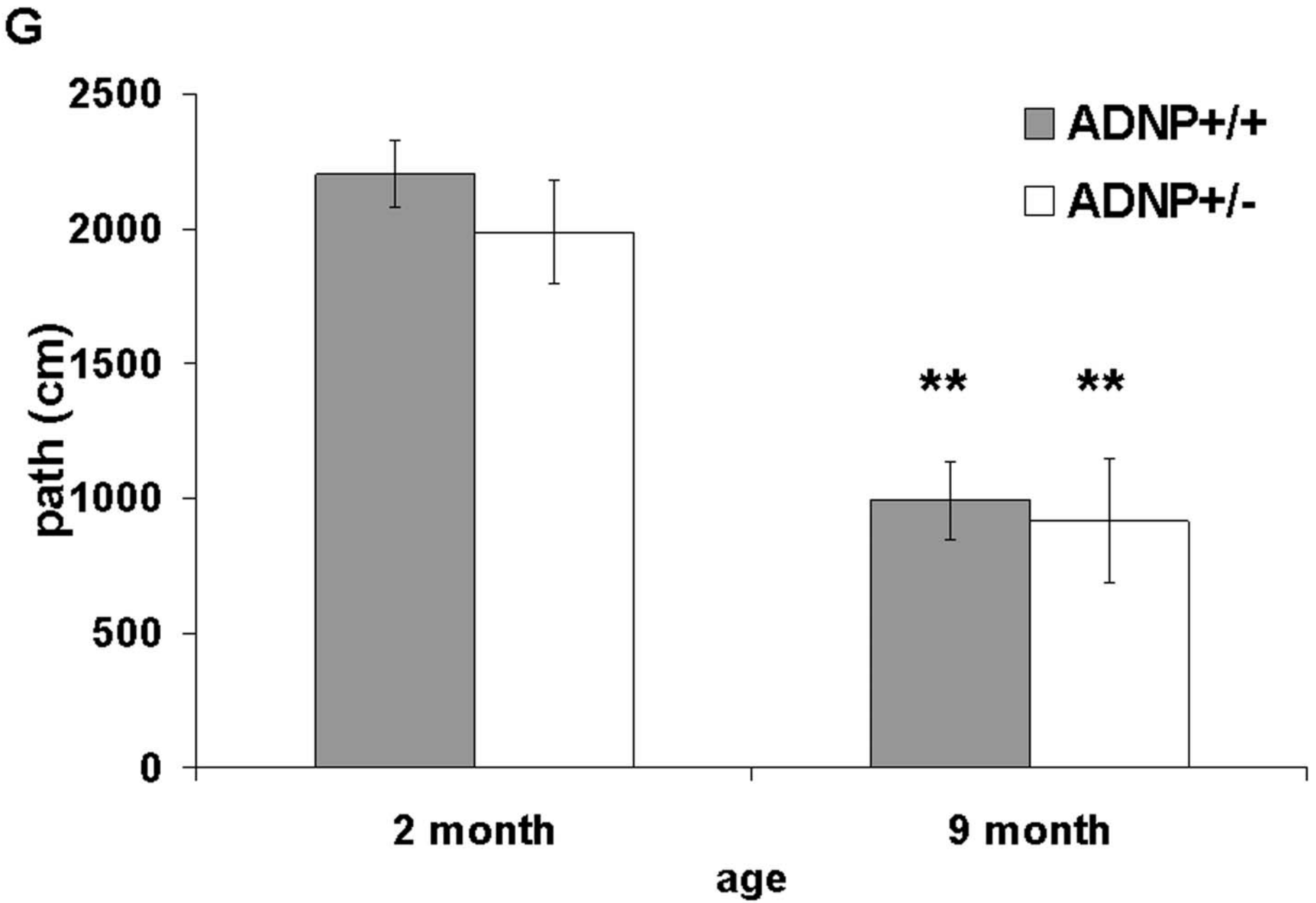

Figure 6H